Review Article

Tuhua Zhong[#], Guoqing Jian[#], Zhen Chen, Michael Wolcott, Somayeh Nassiri*, and Carlos A. Fernandez*

Interfacial interactions and reinforcing mechanisms of cellulose and chitin nanomaterials and starch derivatives for cement and concrete strength and durability enhancement: A review

https://doi.org/10.1515/ntrev-2022-0149 received December 6, 2021; accepted June 14, 2022

Abstract: Nanomaterials have been widely researched for use in construction materials. Numerous studies demonstrate that nanomaterials in small quantities can significantly improve the macroscopic properties of cement paste, mortar, or concrete through various mechanisms. Nanomaterials retrieved from biomass sources have recently gained particular research interest due to remarkable structural properties and the source material's abundance and renewability. Cellulose and chitin are the most abundant polysaccharides in nature; thus, they are candidates for

nanomaterials extraction as multifunctional additives in cementitious systems. In recent years, cellulose nanomaterials in cementitious composites have been extensively investigated, but chitin nanomaterials and starch derivatives for cement and concrete are still emerging research areas. This review article starts with an overview of polysaccharide nanomaterials' (PNMs) physicochemical properties as a result of different chemical and mechanical extraction processes. Next a brief overview of cement hydration chemistry and microstructure and the interfacial interactions between the cement and the various surface chemical functionalities of PNMs are discussed. Then, the key mechanisms governing the cement strength enhancement by PNMs, such as bridging, nucleating and filling effect, and internal curing, are described. Finally, the impacts of PNMs on other properties of the cement are discussed.

Keywords: polysaccharide, cement, cellulose, chitin, mechanical properties, nanocrystal, nanofibers

Tuhua Zhong: Composite Materials & Engineering Center, Washington State University, Pullman, WA 99164, United States of America; Institute of New Bamboo and Rattan Based Biomaterials, International Center for Bamboo and Rattan, Beijing 100102, China Guoqing Jian: Pacific Northwest National Laboratory, Richland, WA 99352, United States of America

Zhen Chen: Department of Civil and Environmental Engineering, Washington State University, Pullman, WA 99164,

United States of America

Michael Wolcott: Composite Materials & Engineering Center, Washington State University, Pullman, WA 99164, United States of America

1 Introduction

Concrete is the most widely used construction material [1]. Increased demand from China, India, the Middle East, Northern Africa, and North America drove the annual global production of cement (the major binder component of concrete) to 4.08 billion metric tons in 2019, with about 86 million tons produced in the U.S. [2]. Concrete is easy to manufacture by proportioning by weight and mechanically mixing the components. Furthermore, it can be made into any desired shape in its fresh state, while some of the cured products gain attractive mechanical properties as early as a few hours [3]. However, CO₂

[#] These authors contributed equally to this work and should be considered first co-authors.

^{*} Corresponding author: Somayeh Nassiri, Department of Civil and Environmental Engineering, Washington State University, Pullman, WA 99164, United States of America, e-mail: nassiri@ucdavis.edu

^{*} Corresponding author: Carlos A. Fernandez, Pacific Northwest National Laboratory, Richland, WA 99352, United States of America, e-mail: Carlos.Fernandez@pnnl.gov

emissions associated with Portland cement production are estimated to be around 5% of the global anthropogenic carbon dioxide [4–7]. Frequent repairs and infrastructure rebuilding are the main drivers of the high demand for concrete to address cracking. The high susceptibility of current concrete to early cracking is a major concern for the long-term sustainability of infrastructures worldwide.

In the last century, Portland cement has been widely used for different infrastructures, but it results in early cracking [8,9] due to large thermal and drying shrinkage deformations, reduced creep, and increased elastic modulus [8]. Cracks allow water/gas/ions to penetrate the structure faster, leading to steel reinforcement corrosion and subsequent concrete spalling [10]. Therefore, concrete infrastructure requires frequent repairs or replacements, increasing $\rm CO_2$ emissions, and energy usage associated with concrete production. To overcome the burden of recurrent failing infrastructure and reduce concrete-associated $\rm CO_2$ emissions, strategies to enhance the durability of concrete, extend infrastructure life cycle, and delay structural repair and replacement while meeting rapid construction requirements are urgently needed.

In recent years, nanotechnology innovations have enabled improving macroscopic properties of concrete by altering the atomic structure of the calcium-silicatehydrate (C-S-H) gel [11]. C-S-H is the key cement hydration product (50-70 wt%) and is responsible for the strength development, physical properties, and durability of concrete [12]. However, shrinkage, creep, restructuring, and microcracking can also develop within the C-S-H gel. Therefore, there is a great interest in modifying the structure and properties of C-S-H to achieve desired performance from the concrete composite. Nanomaterials can offer multiple unique advantages such as densification and reinforcement of the C-S-H gel, altering its degree of polymerization (DP) [13] and silica mean chain length of C-S-H [14], and increasing the stiffness of C-S-H [15]. Other effects from nanomaterials on the cement properties have been speculated from the creation of additional nucleation sites to facilitate extra hydration reactions, reduced porosity, and refinement of the cement pore structure [16]. Consequently, improvements in performance, such as subsequent reduction in chloride permeability, have been reported [17,18]. Furthermore, it has been shown that nanomaterials can greatly enhance current ultra-high-performance concrete by reducing cement usage and mitigating their excessive shrinkage and cracking issues [19].

The most researched nanomaterial for cement composites is carbon nanotubes (CNTs), which have demonstrated

tremendous abilities in boosting cementitious systems' mechanical and durability properties. However, wide stream use of CNTs in concrete-based construction is not possible until many challenges associated with CNT manufacturing are overcome to significantly reduce their cost and increase their availability in larger amounts. In addition, due to their inert surface chemistry, CNTs require surface functionalization for good dispersion and interfacial chemical compatibility and reactivity with cement [20-22]. Additional treatments and dispersion processes could add to the complexity of concrete production with nanomaterials, concrete cost, and the overall CO₂ footprint of concrete production. In order to develop the cost-effective and scalable nanomaterials which can be globally adopted to reduce energy consumption and CO₂ emissions of concrete, the nanomaterials should have the following characteristics:

- 1) Abundant feedstock resources;
- 2) Scalable and low-energy extraction/manufacturing methods,
- Convenient dispersion, placement, finishing, and cleanup to maintain construction efficiency and promote implementation by concrete suppliers, builders, and project owners.

Biobased additives from abundant biopolymers in the nanoscale have received significant attention from researchers in recent years. Nanomaterials derived from cellulose (the most abundant biopolymer) have shown great potential for use in the cement industry [23-25]. However, less focus has been on chitin as a source for nanomaterials, though chitin is the second most abundant polysaccharide biopolymer [26,27] after cellulose. Other polysaccharides, e.g., starch and its derivatives, are only reported in a few studies [28,29]. Derivatives and nanostructures from these environmentally friendly biopolymers could offer cost-effective and low-energy alternatives to CNTs if sufficient study is carried out for cement and concrete use, providing their manufacturing processes are streamlined. Therefore, this review article aims to turn on the spotlight on these underused biopolymers for nanomaterials extraction for cementitious systems. Furthermore, the effects of polysaccharide nanomaterials (PNMs) on the properties of cement and concrete greatly vary depending on the nature of polysaccharides and the characteristics of PNMs, including surface chemistry, size, morphology, surface charge, etc. The impact of these properties on interfacial interactions with cement and consequential effects on concrete performance has been overlooked in current cement and concrete literature. Therefore, this manuscript aims to give readers an overview of the applications and the ensuing effects and

probable reinforcing mechanisms of different types of polysaccharides and their nanomaterials in cement and concrete. This review also aims to draw the attention of researchers to knowledge gaps and areas of future research needed to expand the use of PNMs in cementitious systems.

To do so, this article first presents a comprehensive review of PNMs, including cellulose, chitin, starch (and its derivatives), and their application in cement and concrete. Recent advances in preparation methods and surface modification for making PNMs are reviewed, and their interfacial interactions with cement, and effects on the mechanical properties of cement and concrete are summarized. The mechanisms for nanomaterial-cement interactions and the factors affecting cement and concrete mechanical properties, such as size, morphology, concentration, and dispersion of nanomaterials, are also discussed.

2 Literature review methodology

The literature review methodology used the following search engines; Google scholar, Google patent, SciFinder, Patentsout, and Baidu. The searched keywords included cellulose cement (concrete), cellulose nanocrystal cement, cellulose nanofiber cement (concrete), chitin cement (concrete), chitiosan cement (concrete), chitin nanocrystal cement (concrete), chitin nanofiber cement (concrete),

starch cement (concrete), polysaccharide cement, among others. The authors reviewed publications and patents reported over the past 30 years.

3 Production methods of PNMs

Emerging biobased PNM additives, particularly cellulose nanomaterials, have been applied in cement and concrete for different end outcomes, *e.g.*, strength enhancement, hydration booster, internal curing, rheological modification, and others. The properties of the PNM-reinforced or modified cement and concrete are usually governed by the characteristics of PNMs, such as their size, morphology, aspect ratio, surface chemistry, charge, *etc.* PNMs' characteristics are determined by the nature of the polysaccharides and the extraction methods. Therefore, the following sections provide an overview of different types and production methods of PNMs.

3.1 Sulfated cellulose nanocrystals

Cellulose is a polydisperse linear polymer of poly- β -(1,4)-D-glucose residues and has a flat ribbon-like conformation [30]. The repeating unit (Figure 1a) is comprised of anhydro-glucose rings $(C_6H_{10}O_5)_n$. Cellulose chains have

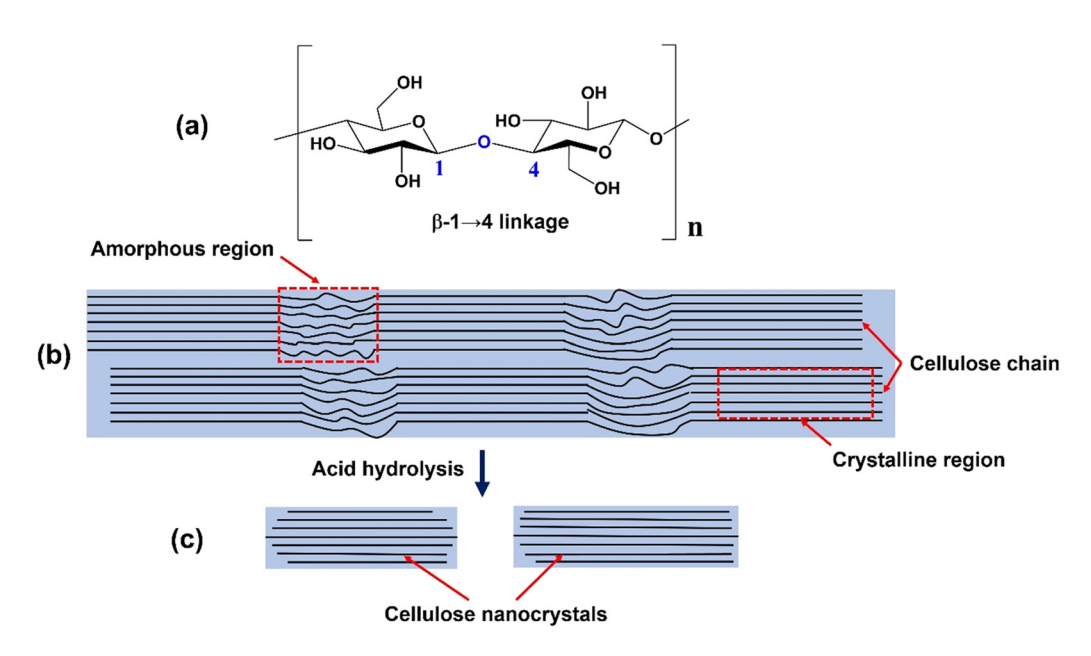


Figure 1: Schematics of (a) repeating unit of cellulose chain with the directionality of the $1 \rightarrow 4$ linkage, (b) idealized cellulose microfibril with one of the suggested configurations of the crystalline and amorphous regions, and (c) cellulose nanocrystals after acid hydrolysis dissolved the disordered regions.

a degree polymerization of approximately 10,000 glucopyranose units in wood cellulose and 15,000 in native cellulose cotton [31,32]. Nanocellulose can be produced in different ways, leading to different properties and dimensions. Two main forms of cellulose nanomaterials can be obtained: cellulose nanocrystals (CNCs) and cellulose nanofibers (CNFs). Tables 1 and 2 summarize the different methods for producing CNFs or CNCs, such as mechanical fibrillation or sulfuric acid hydrolysis using wood pulp for producing CNFs [33-37]; 2,2,6,6-tetramethylpiperidine-1-oxyl radical ((TEMPO)-mediated oxidation and followed with mild disintegration in water) using wood pulp [38-41] for producing CNFs; and sulfuric acid hydrolysis with wood pulp, cotton fibers, algae, wood chips, pulp sludge, among other precursors for producing CNCs [42-46].

CNCs and CNFs, as shown in Figure 1, have distinct physical and chemical properties. For instance, CNCs have a higher degree of crystallinity than CNFs. In addition, CNCs exhibit rod- or whisker-like structures, while CNFs are typically fibrous and include amorphous regions [47].

CNCs are usually isolated from semi-crystalline cellulose fibers using a strong sulfuric acid hydrolysis process in which the amorphous region is digested and the crystalline region is intact. Thus, individual crystallites with a little amorphous phase remaining (CNC has high crystallinity of ~80%) are released with the assistance of mechanical disintegration processes (e.g., ultrasonication), as represented in Figure 2b and c [48]. Sulfuric acid is one of the widely used inorganic acids for the hydrolysis process because of its low cost and its reactivity with the hydroxyl groups on the surface of crystallites; thus, it can introduce anionic sulfate groups. The resulting cellulose nanocrystals are often referred to as sulfated cellulose nanocrystals. These negatively charged sulfate groups play an important role in stabilizing CNCs in water due to interfibrillar electrostatic repulsion forces [48]. Sulfate cellulose nanocrystals are mainly prepared from wood pulp due to abundant resources and low cost. The resulting cellulose nanocrystals exhibited rod-like or spindle-like shapes and have a diameter of 3-5 nm and a length of 50-500 nm [30,48]. Strong acid hydrolysis treatment results in hydrolysis of the glycosidic bonds of cellulose, especially in the amorphous region, thus reducing the DP. It was reported that the DP of cellulose from bleached wood pulp ranges from 140 to 200 [49]. The number of sulfate groups depends on the hydrolysis time and sulfuric acid concentrations. The sulfate content of the resulting sulfated cellulose nanocrystals was about 0.2–0.3 mmol/g CNCs [50–52]. Therefore, there are still a certain number of hydroxyl groups co-existing with sulfate groups on the surface of the sulfated cellulose nanocrystals, as shown in Figure 2(b) and (c).

3.2 Carboxylated CNFs

The TEMPO-mediated oxidation is regarded as one of the most effective pretreatment processes of cellulose fibers because it can selectively oxidize primary C-6 hydroxyl groups into anionic carboxylate groups (-COO⁻) under alkaline conditions [53]. This TEMPO-mediated oxidation reaction occurs on the surface of cellulose fibers and in their amorphous regions. As the carboxylate content increases to a certain amount, cellulose begins to disperse in an aqueous solution [53]. The negative charges can induce interfibrillar electrostatic repulsion forces and thereby facilitate nano-fibrillation in the subsequent mechanical separation process resulting in the production of fine and individualized CNFs with a diameter of 3-4 nm, a length of microns, and an aspect ratio greater than 100 [54,55]. The resulting carboxylated CNFs are often referred to as TEMPO-oxidized CNFs (TOCNFs). Compared to the acid-hydrolyzed cellulose nanocrystals, TOCNFs have much higher shear stress and viscosity due to the relatively higher aspect ratio, higher dispersibility, and fewer bundles in water [53]. The carboxylate content on the cellulose surface is highly dependent on the concentration of the oxidant sodium hypochlorite (NaClO). When the NaClO concentration in the TEMPO-mediated oxidation process increases from 2 to 5 mmol/g-pulp, the carboxylate content increases from 1 mmol/g-CNF to about 1.3 mmol/g-CNF. However, the DP decreases from 1,000 to 520 [55]. As mentioned earlier, TEMPO-mediated oxidation only takes place on the surface of CNFs. In the amorphous region of CNFs, most of the hydroxyl groups on the C2 and C3 remain intact. Thus, there is a high density of hydroxyl groups co-existing with carboxylate groups on the surface of TOCNFs, as shown in Figure 3.

3.3 Mechanically fibrillated CNFs

The mechanical fibrillation method does not involve any chemical treatment; it is less effective in de-fibrillation of cellulose fibers into nanofibers than chemical processes (i.e., strong acid hydrolysis and TEMPO-mediated oxidation). However, it may benefit from lower manufacturing costs and no chemical usage to alleviate the environmental burdens compared to the TEMPO-mediated oxidation method for CNFs and the strong sulfuric acid hydrolysis method for CNCs. A friction grinding process is usually applied for the

 Table 1: Cellulose nanofibril-reinforced cementitious materials

CNF; Source: wood pulp; Production method: mechanical; 0–0.4 wt% of cement Diameter: 20–200 nm; Length: 1–2.5 μm CNF; Source: wood pulp; Production: TEMPO oxidation; 0–0.4 wt% of cement Diameter: 50–90 nm; Length: 400–800 nm			rel.
	nt General use limestone cement	 106% improvement in fs 184% improvement in energy absorption 10% increase in the hardness 	[33]
	ordinary Portland cement (OPC) (PII 42.5R)	 20% increase in Cs 15% increase in fs Initial setting time increases from 170 min to 272 min and final setting time increases from 219 min to 310 min 	[40]
CNF; Source: wood pulp; Production: 48% sulfuric acid 0.04 wt% of cement hydrolysis: Diameter: 20 nm: Length: several microns	t Oil well cement (OWC)	/ 23.9% increase in fs	[34]
CNF; Source/method: wood pulp with 48% sulfuric acid 0.04 wt% of cement hydrolysis followed by homogenization; Diameter: 20–30 nm; Length: several hundreds of microns; Aspect ratio: over 1.000	t OWC	 / fs was increased from 11.24 to 13.63 MPa / Cs was increased from 39.57 to 39.64 MPa after the addition of 0.04 wt% CNF 	[35]
Nanofibrillated cellulose (NFC); Source: eucalyptus pulp; 0.3 wt% of cement Production method: bleaching process and deproteination and demineralization; Diameter: 5–10 nm; Length: several microns; Carboxylate content: 0.5 mmol/g fiber	Type I cement 32.5 N EN197-1:2,000 w/c = 0.26	 36% reduction in porosity 43% increase in Cs 36% improvement in thermal conductivity Both the initial and the final setting times have decreased as NFC contents increase 	[41]
Cellulose filament; Source: wood pulp; Production: 0.05, 0.1, 0.15, and 0.2 wt% mechanical method; Diameter: 10–400 nm; Length: 100–2.000 microns	0.2 wt% Type I cement (ASTM C494 + class F-fly ash	\checkmark Decreased $\it Cs$ while increased $\it fs$	[36]
Bleached Chemi-Thermo-Mechanical Pulp (Aspen, grade 0–1.18% CNF (kg/m³ paste) 325/85/100 H T) was used as the source for the CNF generation by TEMPO method; Diameter:10–20 nm; Length: a few microns	1 ³ paste) Portland cement type II	 Addition of CNF increased the yield stress from 11.36 to 22.09 Pa at 0.2% CNF and to 71.06 Pa at 0.8% CNF The viscosity increased only from 0.54 to 0.68 Pa s and to 1.26 Pa s by addition of 0.2 and 0.8% CNF, respectively 	[38]
CNF by InnoTech Alberta; Source: bleached chemo- 0-0.185 wt% of cement thermomechanical wood pulp; Production method: TEMPO oxidation followed by Supermass Colloider; Diameter: 5-20 nm; Length: a few microns; Carboxylate content: 0.13 mmol/g fiber	nent Portland cement type GU	alleviated bleeding and shrinkage at early dration dration upon adding CNF ress of deleterious agents into cement seree of hydration (DOH)	[39]
CNF; Source: wood pulp; Production method: mechanical 0.015, 0.03, 0.06, 0.09, and fibrillation; Diameter: 20–50 nm; Length: typically, less 0.15 wt% of cement than 0.2 mm; Zeta potential: –34 mV at pH = 7	0.09, and Portland cement type I/II	 3–31% improvement in 7 days Cs 39–116% improvement in fs 49 and 26% reduction in autogenous shrinkage for 0.06 and 0.00 wt% CNF rement respectively 	[37]
CNF; Source: wood pulp; Production method: mechanical 0.1–0.8 wt% of cement fibrillation; Diameter: 25 and 500 nm; Length: several microns	nent OPC	Addition of CNF between 0.1 and 0.2 wt% led to a general increase in the modulus of rupture and modulus of elasticity values	[73]

(Continued)

	1		
	Ġ	ì	
_	\$:	
,	i		
	\$		
	•		
١	•		
	•	•	
1	۰		
		j	
•	•		
	(ī	
		A. Continu	Continu

PNM type/source/production/size	Nanocellulose dose	Cementitious material	Effects on mechanical properties	Ref.
CNF; Source: wheat straw; Production method: prepared by HCI, NaOH, peracetic acid pretreatments of wheat straw followed by sonication (30 min) treatment; Diameter: 150–400 nm; Length: several microns	0.5, 1, 1.5, and 10 wt% of cement mortar	Not provided	$^{\prime}$ Improved Cs by 27% at an optimum dosage of 0.5 wt%	[74]
CNF; Source: N/A; Production method: N/A.	0.025, 0.05, 0.1, 0.3, and 0.5% (solids) by weight of cement	OPC type I/II	At 90 days, 0.05% CNF in cement paste resulted in 24 and 15% increase in the Cs of cement paste with 0.35 and 0.45 w/c, respectively fs of cement paste increased up to 75 and 55% due to the addition of 0.5% of PCNF and nano silica-CNF, respectively	[75]
CNF; Production method: mechanically fibrillated cellulose from University of Maine; Diameter: 28.2 ± 20.8 nm; Length: several hundreds of microns	0.065 wt% by weight of cement Type I/II OPC	Type I/II OPC	Max% increase in 7 days and 28 days Cs 17 and 18%, [76] with 0.065 wt% CNF 0.065 wt% CNF 0.065 wt% CNF enhanced E by 40% Concentrations of CNF resulted in 0 to a maximum of 21 min delay in the initial set time of the control 0.075 wt% CNF cement showed a faster initial setting than the control Three concentrations of 0.045, 0.05, and 0.055 wt% delayed final setting times by 15, 39, and 56 min In the first 90 min period, all CNF-cements showed similar or slightly higher consistency than the control and much higher values than the control +	[92]
CNF; Production method: N/A; Diameter: 5–20 nm; Length: from 50 to >2,000 nm in length	0.15 kg/m³ of concrete	Type I cement	Slight improvements of Cs and fs were observed for curing times longer than 28 days	[77]

 Table 2:
 Cellulose nanocrystal-reinforced cementitious materials

PNM type/source/production/size	Optimal nanocellulose dose	Cementitious material	Effects on mechanical properties	Ref.
CNCs; Source: wood pulp; Production method: sulfuric acid hydrolysis; Width: 3–5 nm; Length: 0.05–0.5 µm; Zeta potential: -64 mV at pH = 7	0.2 vol% of cement	Type V cement	7 20-30% improvement in fs	[42]
CNCs; Source: wood pulp; Production method: sulfuric acid hydrolysis; Width: 3–5 nm; Length: 0.05–0.5 µm; Zeta potential: -64 mV at pH = 7	1.5 vol% of cement	Type V cement	50% improvement in reduced modulus	[43]
CNCs; Source: N/A; Production method: Blue Goose Biorefineries Inc.; Width: 90 nm; Length: 500 nm; Zeta potential: -33.4 mV	0.8 wt% of cement	Type I/II Portland cement	/ Increased fraction of high-density of C–S–H	[78]
CNCs Production: Kraft pulp sourced from Alberta's pulp and paper mill; Width: 5–10 nm; Aspect ratio: 10–60; Zeta potential: N/A	0-0.44 wt% of OWC	Type G cement	/ Improved Cs and fs by 60%	[45]
CNCs; Source: wood pulp; Production method: mechanical fibrillation; Width: 13–335 nm; Length: 100–400 nm	0.1-0.8 wt% of cement	0 PC	 Reduced porosity by 30% Addition of CNC between 0.1 and 0.2 wt% led to a general increase in E and fs 	[73]
CNCs; Source: wood pulp, cotton fibers, algae, wood chips, and pulp sludge; Production method: sulfuric acid hydrolysis; Width: 3-5 nm; Length: 0.05-0.5 μm; Zeta potential: -64 mV at pH = 7	0.023–3.311 vol% of cement	Type I/II and type V cement	V Reduced yield stress by up to 54% at low dosage (<0.2%)	[44]
CNCs; Source: Oil Palm Empty Fruit Bunch; Production method: 0.2 N HCl at 105° C/15 min, microcrystalline cellulose powder mixed with 64 wt% ${\rm H_2SO_4}$ at 45° C/60 min and constantly stirred to produce CNCs; Zeta potential: -50.4 mV	0.4 vol% of cement	Portland cement type I	 Increased yield stress by 10 times at high dosage (1%) Increased Cs by 43–46% 	[46]
Source: any material which comprises a substantial proportion of cellulose; Production method: redox reaction (NaClO with iron sulfate or copper sulfate as a catalyst with buffer) → alkaline extraction → 2nd redox reaction (NaClO with copper sulfate as a catalyst with buffer) → washing and concentrate-CNC; Width: 2.5 mm. Holiett, 5.2 00 mm.	1–5g/kg of cement	Cement type GU	 Substantial increase in fs Marked increase on 3 days, and 30 days, Cs and fs 	[62]
			Initial set time: 289 min without CNC and 409 min with 1g CNC/1 kg cement with superplasticizer and air entrainer	
Bacterial nanocellulose; Source: derived from cellulose obtained from the aerobic fermentation of bacteria of the genus Gluconacetobacter	0.05, 0.1, 0.15, and 0.2 wt% of cement	Class G Portland cement	/ Increased Cs at 28 days but decrease Cs at 7 days for 0.15% bacterial nanocellulose-cement samples	[80]
CNCs by CelluForce; Production method: sulfuric acid hydrolysis; Width: 6 ± 3 nm; Length: 127 ± 59 nm; Zeta potential: -47.5 ± 2.31 mV at pH = 7.4	0.40wt% of cement	Type I/II OPC	/ Max increase in 7 days and 28 days <i>Cs</i> was 9 and 17% at 0.4 wt% CNC, respectively	[92]
CNCs; Production method: N/A; Width: ~5 nm; Length: 50–500 nm	0.15 kg/m³ of concrete	Cement type I	 0.4 wt% CNC increased E by 20% Slight improvements in Cs and fs for curing times longer than 28 days 	[77]

Figure 2: (a) Chemical structure of unmodified cellulose; (b) chemical structure of sulfated cellulose; (c) scheme of rod-shaped sulfated cellulose nanocrystals with hydroxyl and negatively charged sulfate groups on the surface.

mechanical pretreatment of cellulose fibers [53]. The grinder often consists of two nonporous ceramic grinding discs with adjustable clearance between the upper and lower discs. While the upper grinding disc is static, the lower one is rotated at high speed. The cellulose fiber slurries are subject to massive compression, shearing, and rolling friction forces when fed into a hopper and dispersed by centrifugal forces into the clearance between the two grinding discs. When the shearing forces are applied to the longitudinal fiber axis of the fibrous materials, cellulose fibers are ground into microand nanofibers [53]. Due to the complicated, multilayered

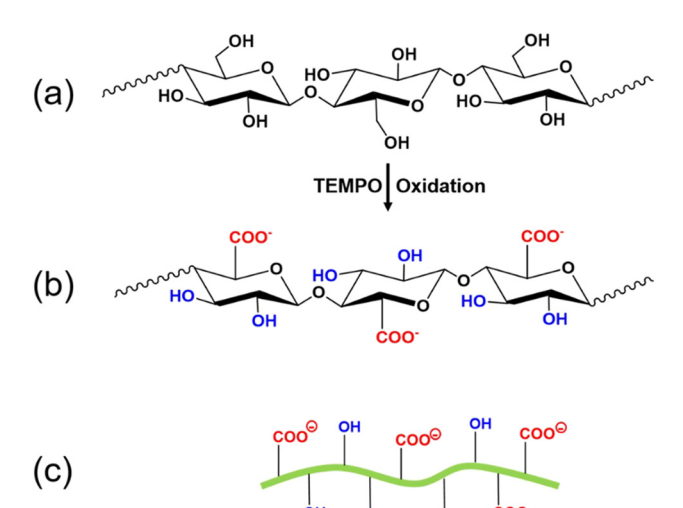


Figure 3: (a) Chemical structure of unmodified cellulose; (b) chemical structure of carboxylated cellulose; (c) scheme of carboxylated CNFs with different groups including hydroxyl and negatively charged carboxylated groups on the surface.

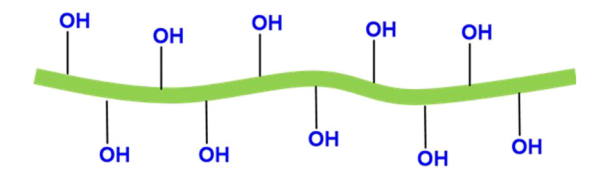


Figure 4: Scheme of mechanically fibrillated CNFs.

structure of plant fibers and interfibrillar hydrogen bonding, the resulting mechanically fibrillated CNFs often include aggregated nanofibers with a wide distribution in width [56]. Thus, mechanically fibrillated CNFs are coarser and larger than TOCNFs [53,56]. Mechanically fibrillated CNFs maintain crystalline and amorphous regions of cellulose chains. CNFs are reported to have a diameter smaller than 100 nm and lengths from 500 nm to several microns [57]. The mechanical fibrillation process by grinding discs will result in a decrease in the DP of the resulting CNFs. The number of the pass of dissolved pulp fibers in the grinder (supermass colloider) increased from 0 to 30. The DP decreased from 750 to about 450 [58]. CNFs produced by the mechanical method show relatively simpler surface chemistry as compared to CNFs obtained by the TEMPO-mediated oxidation method. That means that hydroxyl groups were only functional groups on the cellulose surface, as shown in Figure 4. However, it was reported that a negative charge was sometimes found on the surface of mechanically fibrillated CNFs. This is likely due to the presence of carboxylic groups in the glucuronic acid of hemicellulose left from the pulping process [53,59].

3.4 Carboxylated chitin nanofibers and nanocrystals

Chitin is a polymer of poly(b-(1–4)-N-acetyl-D-glucosamine), which is structurally similar to cellulose, but has acetamide groups at the C-2 positions, as shown in Figure 5a [60,61]. The degree of acetylation (DA) of chitin is typically around 0.90 with additional 5-15% amino groups due to deacetylation during extraction [62,63]. Due to chemical structural similarity, the extraction methodologies of nanofibers from cellulose are similar to that from chitin. In our current study, the TEMPO-mediated oxidation process has been applied to chitins. During the TEMPO-mediated oxidation process, the primary C-6 hydroxyl groups on the chitin surface or in amorphous regions can be selectively oxidized to carboxylate groups [64]. Most of the TEMPO-oxidized cellulose nanomaterials derived from bleached wood pulp exhibit a length of several microns and an aspect ratio of greater than 100, although the length and DP decreased with the increasing addition of oxidant NaClO in the

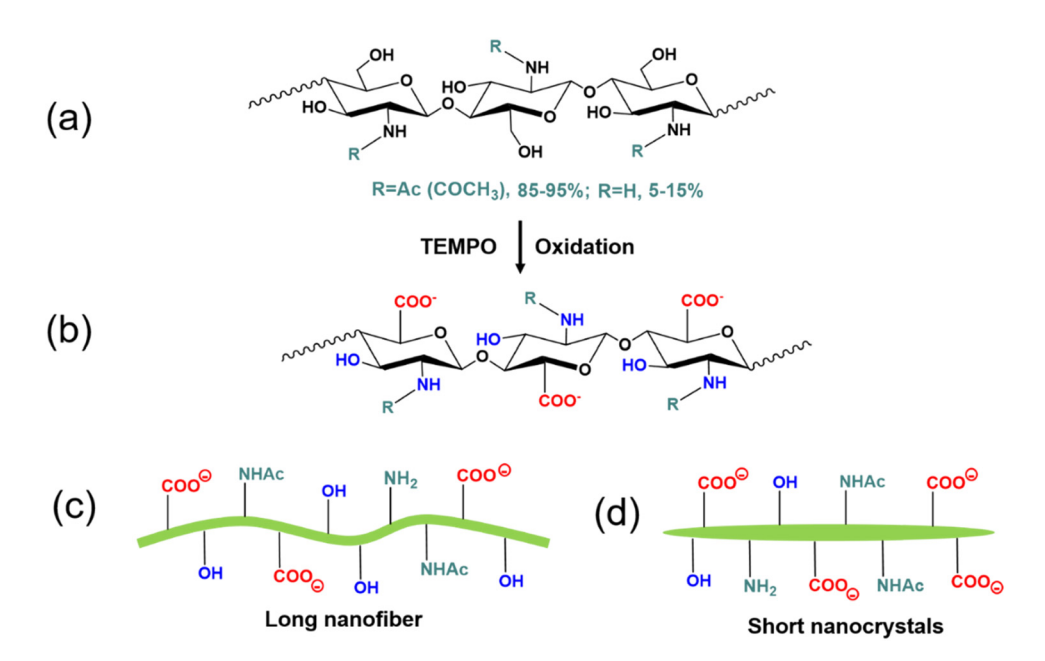


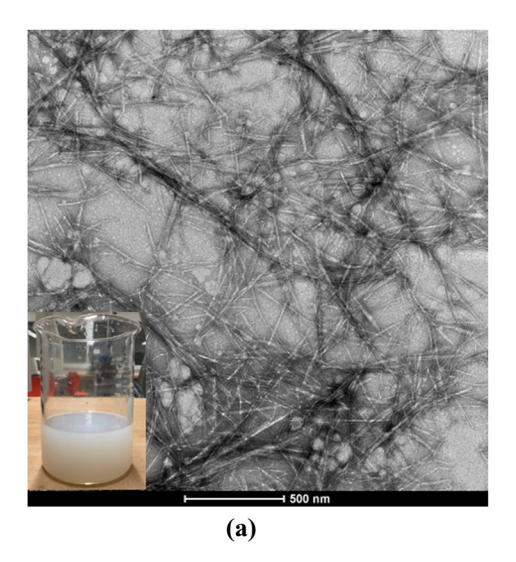
Figure 5: (a) Chemical structure of unmodified chitin; (b) chemical structure of carboxylated chitin; (c) scheme of carboxylated chitin nanofibers with a low degree of oxidation; (d) scheme of carboxylated chitin nanocrystals with a high degree of oxidation.

TEMPO-mediated oxidation process [55,65]. The amount of oxidant NaClO plays a key role in changing the morphology of the chitin nanofibers derived from shrimp shells. We found that when NaClO increased from 3 to 9.5 mmol NaClO/g-chitin, the chitin nanofiber suspensions changed from opaque to transparent suspensions, as shown in Figure 6. The surface chemistry of carboxylated chitin nanofibers or carboxylated chitin nanocrystals is more complex than that of carboxylated CNFs due to the existence and distribution of the acetamido groups or amine groups at the C-2 position, as shown in Figures 5b and 7b. In our experiments, long and aggregated chitin nanofibers were obtained for a low dosage of NaClO, while short and rod-like

chitin nanocrystals were obtained for a high dosage of NaClO (as schematically depicted in Figure 6c).

3.5 Partially deacetylated chitin nanofibers

Alkali hydrolysis is a conventional method for producing chitin with positively charged surfaces, as displayed in Figure 7. The variables (*e.g.*, reaction temperature, reaction time, alkali concentration, *etc.*) during a typical process can be tuned to control the degree of deacetylation to prevent severe degradation of the crystalline structure. Fan *et al.* [66] reported that α -chitin was partially deacetylated with



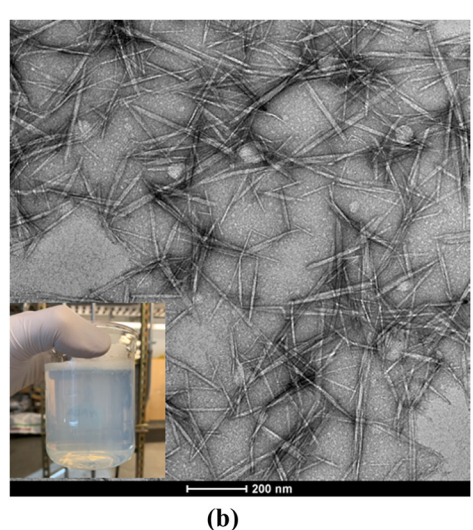


Figure 6: (a) TEMPO-oxidized chitin nanofibers (3 mmol NaClO/g chitin); (b) TEMPO-oxidized chitin nanocrystals (9.5 mmol NaClO/g chitin).

Figure 7: (a) Chemical structure of unmodified chitin; (b) chemical structure of partially deacetylated chitin; (c) scheme of partially deacetylated chitin nanofibers with protonated amino groups at pH 3-4.

a degree of N-acetylation (DNAc) around 0.74-0.70 in the presence of 33% sodium hydroxide (90°C for 2-4 h). The yields of the products are around 85-90%. There is no change in the crystallinity index and crystal size of the α chitin, indicating that most of the deacetylation occurred on the α-chitin crystallite surfaces. After partial alkali deacetylation, acetamido groups in chitin molecules can be converted into amino groups, which can be further protonated under mildly acidic conditions [66], as shown in Figure 7. Positively charged surfaces can facilitate the stable dispersion of chitin nanofibers in acidic water by interfibrillar electrostatic repulsion. It should be noted that pH 3-4 of the dispersing medium was required to ensure protonation of the C2-NH₂ groups in partially deacetylated chitin [66]. It is not unclear whether these partially deacetylated chitin nanofibers can be used in alkali cement systems since the pH of pore solution for cement is often 12 or higher. In such alkaline conditions, the C2-NH2 groups in the deacetylated chitin nanofibers may not change; however, the surface charge of chitin nanofibers will drop significantly, which ultimately can lead to the agglomeration of the chitin nanofibers.

3.6 Mechanically fibrillated chitin nanofibers

The fully mechanical fibrillation process using grinding discs has been applied to generate nanofibers without changing the chemical structure of chitin. However, the

density of hydroxyl groups and amine groups are increased due to the significant increase in the surface areas of chitin nanofibers after ultra-fine grinding. As shown in Figure 8b, the amino groups within mechanically fibrillated chitin nanofibers can be protonated with the addition of acid at a pH of 3–4. This process makes chitin nanofibers positively charged in an acidic aqueous medium. There is no doubt that the positive surface charges of mechanically fibrillated chitin nanofibers are lower than those of partially deacetylated chitin nanofibers because partial deacetylation via NaOH hydrolysis yields more amino groups (-NH₂). In our previous research [67], we successfully produced mechanically fibrillated chitin nanofibers with an average diameter of 12 nm using planetary ball milling as pretreatment and further high-pressure homogenization. These mechanically fibrillated chitin nanofibers also exhibited a positive charge in solution, as evidenced by the zeta potential of about 39 mV at a pH of 3.

3.7 Starch and starch derivatives

Amylose and amylopectin are the two main components of starch. Starch has a similar structure to cellulose and chitin. Natural starch consists of 10–30% amylose and 70–90% amylopectin. Amylose is a linear polysaccharide with D-glucose units and the α -1,4-glycosidic linkages. Amylopectin is a branched-chain polysaccharide with glucose units linked primarily by α -1,4-glycosidic bonds

Figure 8: (a) Chemical structure of unmodified chitin; (b) scheme of mechanically fibrillated CNFs with protonated amino groups at pH 3-4.

or occasionally by α -1,6-glycosidic bonds, which are responsible for the branching. Amylose is similar to cellulose, but glucose units in cellulose are joined by β -1,4-glycosidic linkages, producing a more extended structure than amylose. This high linearity allows multiple hydrogen bonding formations between hydroxyl (–OH) groups which helps dense packing of nanofibers.

There are several publications describing the use of starch in cement [28,68-72]. Dewacker [28] used unmodified starch as a substitute for cellulose to increase water retention in cement and found adding low-cost starch is beneficial for water retention, rheology improvement, and shear bond strength increase. Peschard et al. [69] found the retardation effect was enhanced with the increase in starch-to-cement ratio. This is particularly true for low molecular weight starch. In their study, five admixtures were chosen to add to conventional cement, including cellulose ether (CE), starch ether (SE), native starch (NS), white dextrin (WD), and yellow dextrin (YD). WD and YD are obtained by dextrinization (break down of starch into dextrin's) of NS by heat and acid treatment. They found that the cement setting was retarded by measuring a reduction in the heat flow of hydration of admixture-modified cement compared to unmodified cement. For cement with YD, the heat of hydration in the first 24 h was reduced from 99 J/g (plain cement) to 9 J/g. Infrared spectroscopy also demonstrated that C-S-H was formed in the first 8 h of hydration for cement modified with CE, while no C-S-H was identified after 8 hs in SE- and YD-modified cement. Vieira et al. [70] investigated the dispersing effect of anionic starch and cellulose on mortar. The starch was processed with a sulfoethylation or a sulfation process. Slump and mortar spread tests showed that sulfoethylation starch (SES) derivatives and starch sulfate (SS) derivatives perform better as dispersants than commercial polycarboxylate (PCE) ethers. The results were explained by the fact that commercial PCE ether has a lower charge density. In addition, due to their

high retardation effect, the 24 h compressive strength (*Cs*) of SES- and SS-modified concrete was only a fraction (0.15 and 0.13 MPa) of that of commercial Glenium 51- and Melment SL-modified cement (26.6 MPa and 27.7 MPa, respectively).

Zhang $et\ al.\ [71]$ studied the effect of starch sulfonate as a water-reducing additive. The fluidity of cement paste significantly increases, particularly with low doses of starch sulfonate compared to commercial product naphthalene sulfonated formaldehyde condensates (FDN). According to the authors, this effect is from the thickness of the adsorption layer of the SS (\sim 5.3 nm) on the cement particle surface being larger than FDN (0.58 nm). Patural $et\ al.\ [68]$ studied seven SEs, including four types of hydroxypropyl starch derivatives and two carboxymethyl-hydroxypropyl derivatives, showing an increase in consistency coefficient and a decrease in water retention values. In Tables 1–3, fs stands for the flexural strength, and Cs is the compressive strength. The letter d is the abbreviation of day. E is Young's modulus.

4 Overview of cement hydration and cement hydration products

Cement hydration is a complex reaction process during which multiple phases are formed. PNMs can disperse in the cement slurry system, adsorb on the cement particles and to each other depending on surface charges, create additional nucleation sites for reaction products growth, affect the kinetics of hydration reactions and accelerate or decelerate on various stages of hydration. Therefore, incorporation of PNMs in cementitious systems depends on the composition and nature of the cement and in determining the ultimate performance of the PNM–cementitious material. Thus, it is important to understand the main factors that influence cement hydration kinetics, cementitious

Table 3: Chitin, chitosan, starch, and their derivatives reinforced cementitious materials

PNM type/source/production/size	Dosage of chitin, chitosan, starch and their derivatives	Cementitious material	Effects o	Effects on mechanical properties	Ref.
Hemicellulose, sulfopropylate, starch sulfopropylate, water-soluble starch sulfoethylate	0.8–1.3 wt% of cement	ASTM specifications C270 and C125	/ Incre	Increased Cs from 2.7 to 6.9 MPa	[81]
A mixture of cold-water-soluble (>90 wt%), unmodified starch and a cellulose	0.25-0.5 wt% of mortar	Portland type 1 cement	N/A		[28]
New polysaccharide derivative (NPD) which has a cellulose principal chain and two functional groups	1–4 wt% of cement	Normal Portland cement	✓ Sheä 174.!	Shear stress increased from 28 to 174.5 Pa/s	[82]
(ionic and hydrophobic)			sma sma Caus Conv V Initii	Increased the viscosity significantly with a small amount NPD Caused less setting retardation than conventional viscosity agents Initial setting is 9 h 33 min for 0.03% NPD, while 12 h 21 min for 0.06% hydroxyethyl cellulose	
Phosphorylated chitin; $M_{\rm w}=2.6-3.9 \times 10^4$ Da	0–14 wt% of cement	Monocalcium phosphate monohydrate and calcium oxide (CaO) or dicalcium phosphate dihydrate and calcium hydroxide [Ca(OH),]	/ Incre / Reta	Increased <i>Cs</i> Retarded setting time from 7 up to 60 min	[83]
NS, WD, and YD; $M_{\rm w}=85,000-25,200,000{\rm Da}$	0.5 wt% of cement	White Portland cement (C1), CPA CEM I 52.5, and gray cement (C2), PMES 42.5	✓ Reta	Retarding ability is: $NS < WD < YD$	[69]
Sulfoethylation of starch, sulfation of starch, carboxymethylation of limit-dextrin, carboxymethylation of LODP-cellulose, hydroxyethylation, and subsequent carboxymethylation of cellulose; Degree of polymerization (DP _w): 56–2,600, which is calculated	0.9–20 wt% solution	Kiefersfelden 42.5R	Α / ν		[70]
from the molecular weignt Mw, of the peracetylated limit-dextrins Five hydroxypropylmethyl cellulose (HPMC) and four	0.27 wt% of dry mix	CEM 1-52.5R	Mole	Molecular weight and the hydroxypropyl	[84]
hydroxyethylmethyl cellulose (HEMC); $M_{\rm w} = 210 {\rm k-J}$,010 kDa Chitin and chitosan were used as additives with protein, aliphatic polyester, a poly(lactide), a poly (glycolide), a poly(e-caprolactone), a poly(hydroxy butyrate), a poly(anhydride), an aliphatic polycarbonate, an orthoester, a poly(orthoesters), a	N/A	N/A	cont adm N/A	content seem to have a lower impact on admixed cement hydration process N/A	[85]
poly(amino acid), a poly(ethylene oxide), or a polyphosphazene; Sizes: microcapsules (several microns to tens of microns)					

Table 3: Continued

PNM type/source/production/size	Dosage of chitin, chitosan, starch and their derivatives	Cementitious material	Effects on mechanical properties	Ref.
SS using corn starch with 83% amylopectin	0–3% in water	0PC 32.5R	 Cement paste with SS can reach maximal fluidity at a lower adsorption amount (5 mg/g) 	[71]
Chitosans with different molecular weights [low molecular weight (LMW), 50–190 kDa; medium molecular weight (MMW), 190–310 kDa; and high molecular weight (HMW), 310–375 kDa, and different deacetylation degrees (92, 80, and 76%, respectively)	0.1 wt% of dried mortar	OPC (CEM II 32.5N)	 Increased viscosity in fresh mortars while retaining more water than plain cement HMW chitosan is the polymer with the greatest retarding ability for heavy metals 	[98]
Three panels of HEMC (named as C and TV), two panels of HPMC (named as J and P), two panels of hydroxyethyl cellulose (HEC, named as H and N). $M_{\rm w}$ (HEMC) = 90–410 kDa; $M_{\rm w}$ (HPMC) = 225–910 kDa; $M_{\rm w}$ (HEC) = 40–2,900 kDa	0.27 wt% of dry mix	Portland cement CEM I 52.5R	 Decreased yield stress as HEMC molecular weight increased Increased consistency coefficient and water retention with higher HEMC, HEC, and HPMC molecular weight 	[88]
Chitosan powder	N/A	Class A special for oil well cementation	/ Epoxy/chitosan-modified cement slurry for use in environmental-friendly acidizing procedures of oil wells	[88]
Two non-ionic chitosan derivatives (hydroxypropyl and hydroxyethyl chitosans) and one ionic derivative (carboxymethylchitosan, CMCH); CMCH with sizes of tens of microns; Negative values of zeta-potential of CMCH	0-0.5 wt% of cement	OPC (CEM II 32.5N)	 Non-ionic derivatives had a weak dosagerelated influence on the fresh-state properties Ionic CMCH showed a more marked effect: acted as a powerful thickener and reduced the workable life of the fresh mixtures, whereas it caused a delay in the hydration of cement. CMCH reduced the slump by 50% 	[82]
Carboxylated, sulfonated polysaccharide with molecular weight from about 500–1,000,000 Da, and a ratio of carboxylate functionalities to sulfonate functionalities from about 0.1–4	0.1–4 wt% of cement	Class H cement	N/A >	[88]
Commercial chitosan powder (84% of deacetylation degree)	A/F-chitosan aqueous suspension (5 wt% of cement)	Class G cement	 Significantly improved chemical stability of cement slurries in the presence of acidizing fluids 	[06]
Water-soluble oligochitosan (CO). $M_{\rm w}=30,183{\rm Da}$	0.4 wt% of cement	OPC, Shengwei 42.5R and Jidong 42.5	 Increased Cs Strong retarding effect on cement hydration Max water-reducing ratio was 43% 	[91]
			(

Table 3: Continued

PNM type/source/production/size	Dosage of chitin, chitosan, starch and their derivatives	Cementitious material	Effects on mechanical properties	rties	Ref.
A PCE-based superplasticizer (SP) and three types of polysaccharide-based viscosity modifying agent (VMA)	0–0.025 wt% of binder (cement + fly ash)	Normal Portland cement (CEM I 42.5N, EN 197)	 The 7 days C_s decreased from 40 MPa to as low as 22 MPa and 28 days C_s decreased from 50 MPa to as low as 32 MPa The addition of VMAs reduced the segregation tendency for all concrete mistures technol. 	from 40 MPa to as 1ys C _s decreased s 32 MPa duced the all concrete	[92]
Chitosans with different molecular weights (LMW, 8–15 kDa; and HMW, 150–200 kDa) and 90–92% deacetylation degree; commercial products from the Naijin industry (Shanghai, China)	0.25, 0.5, and 1 wt% of the cement weight	Class G OWC	LMW and HMW chitosan reduced fs of cement paste Chitosan has retarding effect. However, after pre-chelating, retarding effect of chitosan will hacome weaker	reduced fs of fect. However, ding effect of	[63]
Chitosan with a size of 74–297 microns Processing chitin with a 40–49% sodium hydroxide aqueous solution under the temperature of 110–140°C for 4–6 h	0.1– 4 wt% of cement 0.2–2 wt% of cement	N/A N/A	/ Retarded setting time significantly / No obvious change in Cs	gnificantly	[94] [95]
Modified LMW chitin polymer	0-0.6% in water	PII 52.5 cement	 Increased Cs from 20 MPa using 0.6% CG-M-chitin Used as SP, reduced the water significantly with the same slumn 	a using 0.6% CG- water significantly	[96]
Modification of chitosan with methacrylic anhydride and crosslinked to ChiMOD hydrogels	0.5, 1, and 2 wt% of cement	OPC (CEM I 52.5N)	 0.5 and 2 wt% of chiMOD hydrogels decreased /5 by 9.6 and 16.7%, and Cs decreased hy 17 and 22%, respectively) hydrogels 16.7%, and <i>Cs</i> 6. respectively	[67]
Oxidation (carboxylic acid converted to hydroxyls) via TEMPO of chitin nanocrystal derivatives and hydrocarbon chitin nanocrystal derivatives and combinations thereof. Amine functional groups are substituted by amide groups. Chitin deacetylation followed by amine functionalities and by acylation;	1–25 wt% in dry cement	N/A	/ Hydrocarbon chitin nanocrystal derivative serves as a rheology modifier, emulsion stabilizer, and fluid loss additive	crystal derivative differ, emulsion additive	[88]
Chitosan-g-POEGMA (Chitosan-g-poly[oligo (ethyleneglycol) methyl ether methacrylate]) graft copolymers	N/A	CEM I 42.5R	 28 days Cs is determined as 30 MPa for the reference concrete, 35 MPa for sulphonated graft, and 34 MPa for sulfonated chitosan within the reference concrete series Maintained better consistencies than those with chemical admixtures during 45 min (sulfonated graft and chitosan) 	as 30 MPa for the Pa for sulphonated fonated chitosan crete series tencies than those s during 45 min tosan)	[66]

Table 3: Continued

PNM type/source/production/size	Dosage of chitin, chitosan, starch and their derivatives	Cementitious material	Effects on mechanical properties	Ref.
LMW chitosan polymer	Polylactic acid $M_{\rm w}=6,000-8,000$ Da, used as alkali silicic acid inhibitor	N/A	✓ Increased Cs and reduced fs	[100]
Chitin-acrylic acid copolymerized multifunctional organic anti-dispersant; <i>M</i> _w : 2,170,000–2,480,000 Da	0.5–2.0% in water	N/A	Cs decreases but with better antidispersion behavior	[101]
nitosan with a low $M_{ m w}$ 29, weight-average	0–0.9 wt% of the paste	γ-C ₂ S	Cs and fs increased by 66% and 299% at 0.6% chitosan content, respectively	[102]
Chitin nanofibers and chitin nanocrystals; Source: chitin from shrimp shells; Production method: TEMPO-oxidation and mechanical fibrillation chitin nanofibers width: 16 ± 10 nm, length: 1,068 ± 765 nm	0.035-0.1wt% of cement	Type I/II OPC	 Chitin nanofibers significantly increased the 28 days fs by approximately 40% at optimum concentrations of 0.05 wt% Chitin nanocrystals delayed initial and final set times by up to 56 and 106 min, respectively, which are greater than the delays of 35 and 78 min by chitin nanofibers Chitin nanofibers increased the viscosity and yield stress of fresh cement paste, but chitin nanocrystals did not impart a notable effect on rheological properties 	[103]

systems' structures, and the properties of cementitious materials. This section provides a brief discussion of cement in terms of composition, cement hydration, pore structure, *etc.*, to help understand the potential interaction of PNMs and cement in the following sections.

4.1 Hydration of clinker

A typical OPC clinker has a composition of 67% CaO, 22% SiO_2 , 5% $A1_2O_3$, 3% Fe_2O_3 , and 3% other components, and normally contains 4 major phases, alite (tricalcium silicate: C_3S), belite (dicalcium silicate: C_2S), aluminate (tricalcium aluminate: C_3A), and ferrite (tetracalcium aluminoferrite: C_4AF). Several other phases, such as alkalis, sulfates, and calcium oxide, are usually present in trace amounts. The hardening of cement results from reactions between the major clinker phases and water. When the cement is mixed with water, various ions are released such as Ca^{2+} , $H_2SiO_4^{2-}$, $Al(OH)_4^-$, OH^- , SO_4^{2-} , etc. The hydration of cement is a time-dependent reaction process in which four major hydration periods can be distinguished [104].

- 1) Initial hydration (minutes): the dissolution of mainly aluminum-rich clinker phases and precipitation of calcium aluminate sulfate hydrates.
- 2) Dormant period (minutes to several hours): hydration rates decrease significantly.
- 3) Main hydration (hours to days): acceleration of dissolution of dominated silicate-rich phases and precipitation of calcium silicate hydrates and calcium hydroxide lead to setting and early strength development.
- 4) Continuous hydration (days to years): further strength development.

C₃S is the primary component of Portland cement, controlling hardening and strength development and the durability of cementitious materials [105]. As a result, C–S–H, which mainly results from C₃S hydration, is the primary hydration product (comprising about 50–70 wt% by mass) and binding phases in hydrated Portland cement [106]. The growth and densification may be highly affected by the dissolution and diffusion of C₃S [107]. C₂S is another component that contributes to the C–S–H hydration products [108].

Despite decades of studies of C–S–H, the relationship between its chemical position and structure remains not fully understood due to its complex structure [109,110]. It is widely reported that C–S–H has layered calcium-silicate crystal structures with linear silicate-"dreierketten"

and different amounts of bound water [110]. Once the calcium-to-silicate (C/S) ratio is described correctly, a number of characteristic structural features and physical properties can be correlated through atomistic simulations [109]. Therefore, the C/S ratio plays a critical role in constructing the chemical structure of C-S-H. There are two widely agreed molecular models for C-S-H gel depending on the C/S ratio: (1) 14 Å tobermorite (C/S ratio = 0.83, interlayer distance 14 Å, molar water content: 42%, as shown in Figure 9) and jennite (C/S = 1.5, molar watercontent: 42%). Both tobermorite and jennite are composed of calcium-silicate layers separated by an interlayer space containing water and calcium. The calcium ions in 14 Å tobermorite form a planar sheet; the calcium layer in the jennite structure is corrugated [110]. In general, the C-S-H structure is imperfect as it is composed of defective and nanocrystalline tobermorite. The defects may include missing bridging silicate tetrahedra (which can result in a decreased silicate chain length), calcium replacing terminating hydroxides, and calcium in interlayer [110].

4.2 Hydration products and pore structure

Cementitious materials are complex multi-component inorganics with multiscale pore systems. The multiphase microstructure of the hydration products in cement mixtures consists primarily of C–S–H, calcium hydroxide (Ca(OH)₂), and a porous phase [78]. The formation of the major hydration product C–S–H often induces a significant volume of internal and nanometer-scale pores, such as small capillary pores and gel pores, as schematically shown in Figure 10 [112]. When dry Portland cement powder mixes with water, hydration reactions are initiated and produce solid hydration

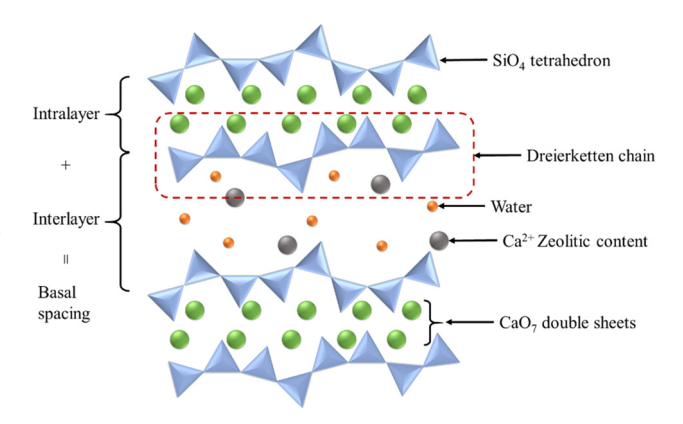


Figure 9: Schematic molecular model of 14 Å tobermorite, reprinted with permission from ref. [111]; Copyright 2020, MDPI.

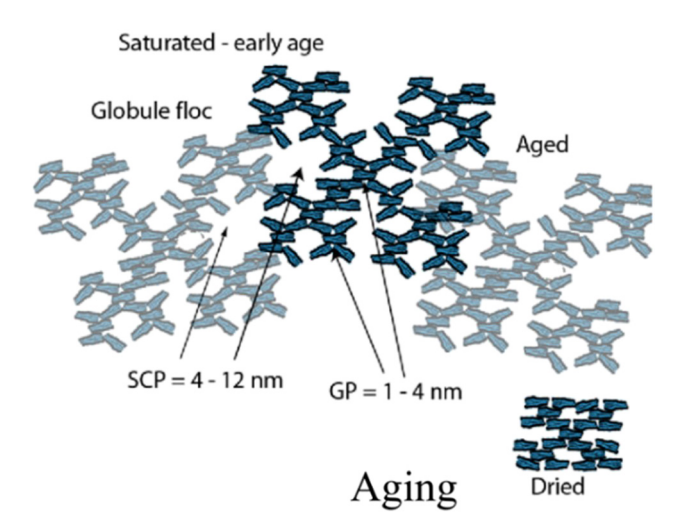


Figure 10: Schematic of particles of C-S-H, referred to as globules or bricks, reprinted with permission from ref. [112]; Copyright 2018, Japan Concrete Institute. They are about 4 nm across and have a layered structure with interlayer space and small pores imperfectly aligned. Their packing arrangement is such that the pores tend to have specific sizes and overall packing efficiency.

products with a greater volume than the initial dry solids. As the hydration continues, the water-filled space is gradually replaced with solids during the reaction. Space not filled by solid hydration products is referred to as the capillary pore space [113]. It has been found that the primary C–S–H gel particles have a lamellar or sheet-like shape with a thickness

of 5 nm and up to 60 nm in width, which is confirmed by transmission electron microscopy (TEM) and atomic force microscopy (AFM) [114,115]. The gel pores are specifically associated with the C–S–H gel phase, the primary hydration product of all Portland cement-based cementitious materials [112].

The nanostructure of cement paste, particularly its nanometer-scale pore system, primarily controls important bulk properties, including strength, shrinkage, creep, permeability, and durability [116]. Particularly, the mechanical properties of the cementitious matrices are influenced by the volume, size, and morphology of pores. High-performance cement requires the capillary porosity to be low [112] because connected pores will allow water to enter the matrix to dissolve hydration products, mainly Ca (OH)₂, thus leading to poor durability [117].

In general, there are two distinct C–S–H hydration regions depending on the volume fraction of gel pores and different modulus in the matrix: (1) low-density (LD) C–S–H and (2) high-density (HD) C–S–H [117]. The first one has a low packing fraction, and the latter has a high packing fraction of nanoscale solid C–S–H particles, as shown in Figure 11, which can be distinguished by a nanoindentation tool [119]. The densities of different C–S–H phases can be determined by nitrogen penetration tests. HD C–S–H is made up of densely packed particles into which nitrogen cannot penetrate. On the other hand, particles of LD C–S–H are not packed tightly, and

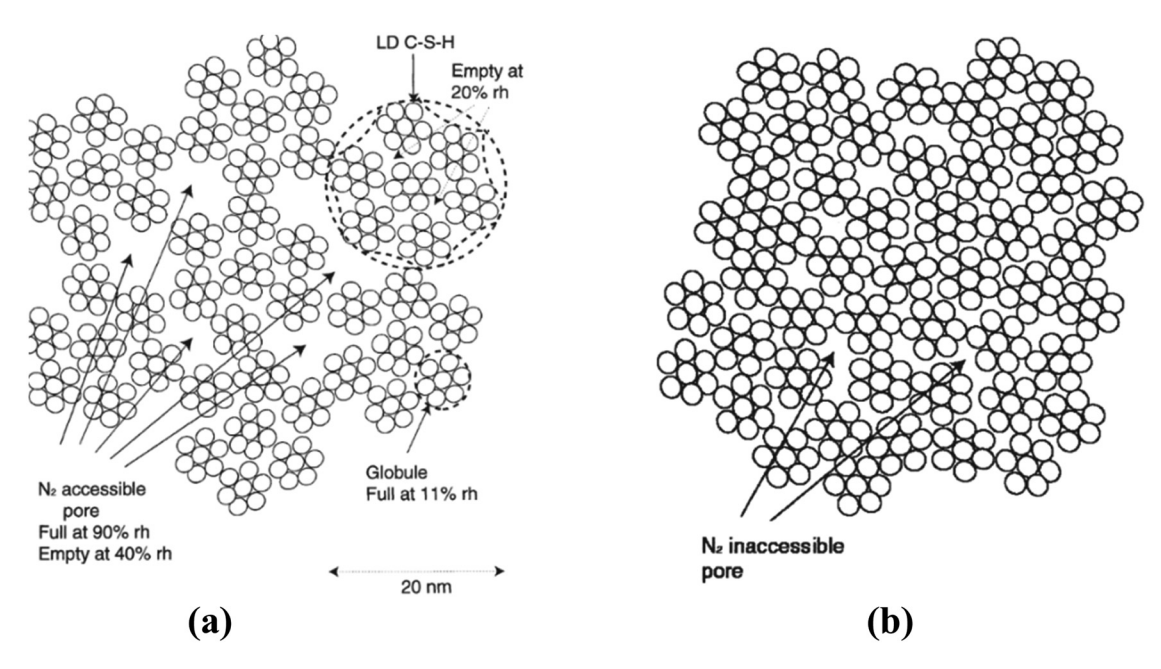


Figure 11: (a) 2D schematic of LD C-S-H formed by the late-stage and/or by drying and (b) 2D schematic of HD C-S-H, the predominant type of C-S-H that forms during the late-stage at water/cement ratio = 0.4, reprinted with permission from ref. [118]; Copyright 2000, Elsevier Ltd.

nitrogen can penetrate partially into this structure, as shown in Figure 11 [118].

Four main factors might govern the structural changes in C–S–H hydration products:

- 1) dissolution and growth of mineral phases,
- 2) diffusion of mobile species in solution,
- 3) complexation reactions among species in solution or at solid surfaces, and
- 4) nucleation of new phases [112].

5 Surface interactions of PNMs with cement

Tricalcium silicate dissolves rapidly in water to release calcium ions (Ca^{2+}), silicon ions (SiO_4^{4-}), and hydroxide ions (OH^-) [105,107]. Once in contact with water, Ca_3SiO_5 is hydroxylated and the surface dissolves according to equation (1); the solution quickly becomes supersaturated with respect to C–S–H, which is less soluble than tricalcium silicate. When the maximum degree of supersaturation is reached, C–S–H precipitates according to equation (2). Because all the calcium ions are not consumed by the precipitation of C–S–H, increasing concentrations of

calcium and hydroxide ions in solution leads to the maximum supersaturation of the liquid phase with respect to calcium hydroxide, which then precipitates as Portlandite, according to the reaction in equation (3):

$$Ca_3SiO_5 + 3H_2O \rightarrow 3Ca^{2+} + 4OH^- + H_2SiO_4^{2-},$$
 (1)

$$\left(\frac{C}{S} + 1\right) Ca^{2+} + 2\frac{C}{S}OH^{-} + H_{2}SiO_{4}^{2-} \rightarrow CSH,$$
 (2)

$$Ca^{2+} + 2OH^{-} \rightarrow Ca(OH)_{2}$$
. (3)

As discussed previously, the C/S ratio plays a crucial role in the chemical structure of C-S-H, and its phase composition and densification may also be affected by the diffusion of calcium ions. Calcium ions have coordination capacity with oxygen atoms of oxygen-containing functional groups and can be attached to negatively charged polymers via electrostatic interaction, as shown in Figure 12 [120,121]. The chemical reactivity and the electrophilic attack of those functional groups decrease in the following order as phosphate > carboxylate > sulfate > hydroxyl [121]. The binding strength of Ca²⁺ with different functional groups decreases in the order of phosphate > carboxylate > sulfate (sulfonate) > hydroxyl because the Ca-O distance (bond length) of the complex of the phosphate is the shortest which ranges from 2.28 to 2.31 Å. The second shortest is the complex of the carboxylate,

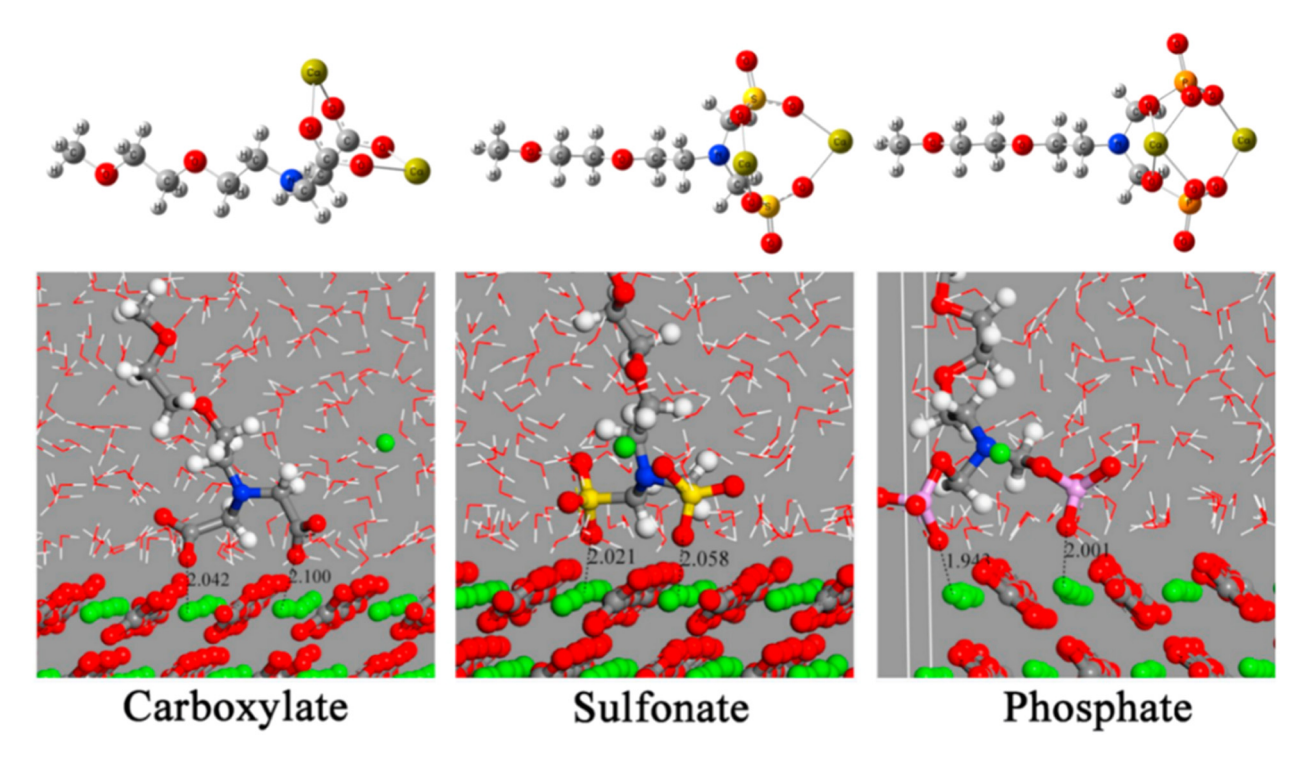


Figure 12: The complexes of three monomers (carboxylate, sulfonate, and phosphate) with Ca²⁺, reprinted with permission from ref. [121]; Copyright 2019, Elsevier Ltd.

around 2.38 Å, which is shorter than that of the complex of sulfate, about 2.42 Å [121,122].

Due to the lack of experimental data and analysis in the literature, it is not well understood about interfacial interaction between PNMs and cement and their influences on the performances of hardened cement composites. The discussion below is mainly based on studies on the interaction between the cement and superplasticizer polymers because superplasticizers contain similar ionic functional groups, particularly sulfate (sulfonate) groups and carboxylate groups similar to those on the surface of polysaccharide nanofibers. It is envisioned that the potential interaction between PNMs and cement may be largely linked to the interfacial interaction of ionic functional groups (anionic sulfate, sulfonate, and carboxylate groups) on the surface of PNMs with the metal cations in the pore solution and cationic compounds.

One of the main functions of superplasticizers is to disperse cement particles. Traditional superplasticizers usually have anionic functional groups, particularly carboxylate and sulfate (sulfonate) groups which can induce the negative charge [123]. Commonly used superplasticizers include sulfonated melamine-formaldehyde condensates, sulfonated naphthalene-formaldehyde condensates,

modified lignosulfonates, and PCE derivatives [124–127], as illustrated in Figure 13.

It is widely accepted that superplasticizers change the dispersion properties of cement through steric hindrance effect and electrostatic repulsion effect [91,123,128,129]. Figure 14 shows a typical structure of a sulfated chitosan superplasticizer. Lv *et al.* [130] proposed the adsorption mechanism of sulfated chitosan superplasticizer (SCS) on cement particles. SCS macromolecules adsorb on cement particle surface by the interaction between various functional groups (-SO₃, -NH₂, -NHSO₃, -OH) in the heterocyclic ring of SCS. The adsorbed SCS results in stronger forces due to steric hindrance and electrostatic repulsion among suspended cement particles, thus improving dispersion ability.

As discussed earlier, the TEMPO-mediated oxidation method is one of the most widely used and also simplest methods to produce carboxylated chitin and cellulose nanomaterials with high yield and crystallinity [64]. While there is no information on the chemical interactions between carboxylated chitin and cellulose nanomaterials and cement, we will refer to research on carboxylate-modified CNTs [131].

Within an acidic solution with a pH of ~2, carboxylate groups are in carboxylic acid form (-COOH). In contrast,

HO
$$\frac{1}{N}$$
 $\frac{1}{N}$ \frac

Figure 13: General structure of (a) sulfonated melamine formaldehyde polycondensates; (b) chemical structure of sulfonated naphthaleneformaldehyde condensates; (c) schematic drawing of the main building blocks of the lignosulfonate molecule; and (d) chemical structure of the polycarboxylate copolymer.

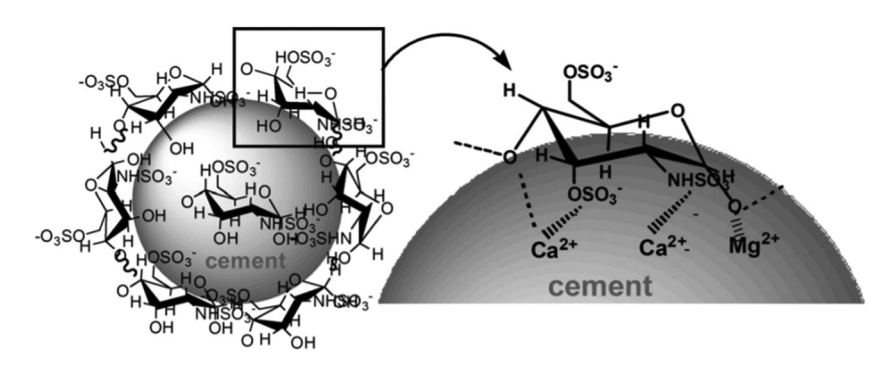


Figure 14: Schematic diagram of the absorption mechanism of SCS on cement particles surface, reprinted with permission from ref. [130]; Copyright 2013, The American Ceramic Society.

within a highly alkaline cement pore solution, carboxylate groups can be fully deprotonated and become negatively charged [125]. In general, the density of negative charges for PCE polymers varies depending on the pH in the pore solution and the molecular structure. The density of negative charges can vary from 20 to 110% when the pH change from 7 to 12.6 [125]. In general, as schematically depicted in Figure 15, there are two forms of coordination bonding between carboxylate groups with Ca²⁺ [125]. As for a monodentate form, Ca²⁺ coordinates with only one oxygen atom of the $-COO^-$ groups in an end-on configuration. In this way, $-COO^-$ is a monodentate ligand for Ca²⁺. As for a bidentate form, Ca²⁺ is bound to both oxygen atoms of a $-COO^-$ functionality in a side-on configuration. So $-COO^-$ is a bidentate ligand for Ca²⁺.

The type of coordination between $-COO^-$ groups and Ca^{2+} depend on the steric accessibility of the carboxylate groups. As shown in Figure 16, for PCE molecules with high side chain density, the carboxylate groups will be shielded by the side chains and the bidentate ligand for Ca^{2+} will be the major coordination type. By contrast, in

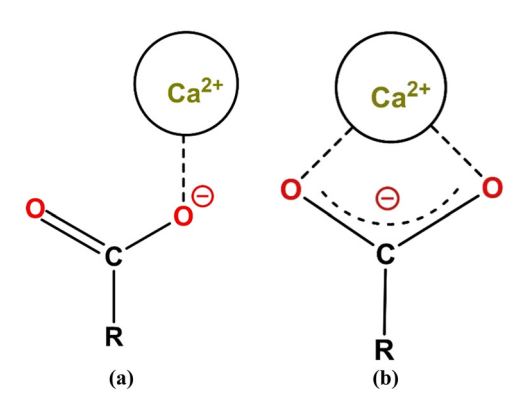


Figure 15: Schematic illustration of two types of coordination between Ca²⁺ and -COO⁻ groups: -COO⁻ as a (a) monodentate; or (b) bidentate ligand.

the PCE molecules containing a high amount of $(-COO^-)$, Ca^{2+} will be coordinated as monodentate [125]. When compared with carboxylate $(-COO^-)$ functionality, the individual metal-oxygen interactions with the sulfonate group are weaker when employed with metal cations. Organosulfonates (RSO_3^-) are primarily regarded as poor ligands by coordination chemists and have been recognized as "non-coordinating" anions [132]. As in the previous discussion, the binding strength of Ca^{2+} with carboxylate groups is stronger than that of Ca^{2+} with sulfate (sulfonate) groups as the chemical reactivity and the electrophilic attack ability of carboxylate groups are stronger compared to sulfate (sulfonate) groups [121,122,133].

Chitosan, a major chitin derivative obtained on an industrial scale by strong alkaline deacetylation, has been used as a chelating agent to remove metal ions in solution because metal cations can be chelated with amino groups (-NH₂) in near-neutral solutions [134]. The amino groups are strongly reactive with metal ions, which is mainly due to the nitrogen atoms of the amino groups (-NH₂) holding free-electron doublets that can react with metal cations [134]. It was reported that amino groups on chitosan have a good affinity for transition metal ions (Zn²⁺, Cu²⁺, and Ag⁺) by chelation mechanisms through the "bridge model" (a transition metal ion is coordinated with four nitrogen atoms of intra- and interchitosan chains) or "pendant model" (a transition metal ion is attached to an amino group of the chitosan chain like a pendant). However, the amino groups (-NH₂) have a very limited affinity for alkali metals (Na⁺ and K⁺) and alkaline-earth metals (Ca²⁺and Mg²⁺) [135–138]. In cement applications, it was known that Ca²⁺ is one of the major ions in the pore solution. It can be inferred that the binding strength of Ca²⁺ with the carboxylate groups on TEMPOoxidized chitin nanofibers (TOChNFs) will be much stronger than that of Ca²⁺ with the amino groups on partially deacetylated chitin nanofibers or mechanically fibrillated chitin

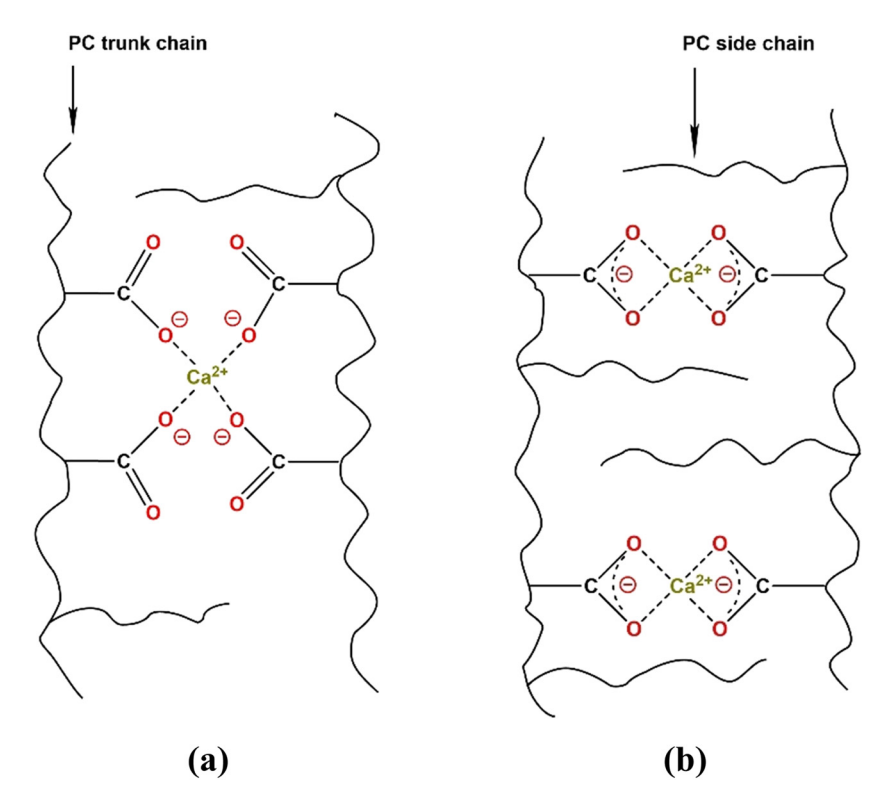


Figure 16: Schematic illustration of (a) monodentate complexation of Ca^{2+} by two polycarboxylate (PC) trunk chains with low side chain density; and (b) bidentate complexation of Ca^{2+} by two PC trunk chains with high side chain density.

nanofibers. Protonated amino groups $(-NH_3^+)$ on chitosan under acidic conditions have a good affinity for anionic compounds [134]. While in the alkaline pore solution in cement, the amino groups $(-NH_2)$ on chitosan are the main reactive groups. Thus, the amino groups $(-NH_2)$ and hydroxyl groups (-OH) will be the dominant functional groups on the surface of these chitin nanofibers.

Based on the above discussions, the possible interactions and states of PNMs with cement might exist as follows:

- 1) intercalation or the formation of an organo-mineral phase (OMP); the formation of OMP often occurs in the presence of nonionic, anionic, and cationic polymers, which can be formed by coprecipitation, intercalation, or micellization [139];
- 2) adsorbed PNMs on the surface of cement particles which help disperse cement agglomerates;
- 3) excess PNMs in the suspensions without chemical or mechanical interaction with cement [139].

5.1 Interactions of sulfated $(-OSO_3^-)$ CNCs with cement

CNCs obtained from sulfuric acid hydrolysis contain anionic sulfate groups (-OSO₃). The sulfate groups within the

sulfated CNCs can interact with metal cations such as Ca^{2+} *via* electrostatic attraction, thus leading to the absorption of sulfated CNCs to the surface of the cement particles. Cao *et al.* [43] reported that about 94.2–96.5% "absorbed" CNCs (aCNCs) have been attached to the cement particles as schematically shown in Figure 17, and the remaining "free" CNCs (fCNCs) were suspended in the pore solution. There

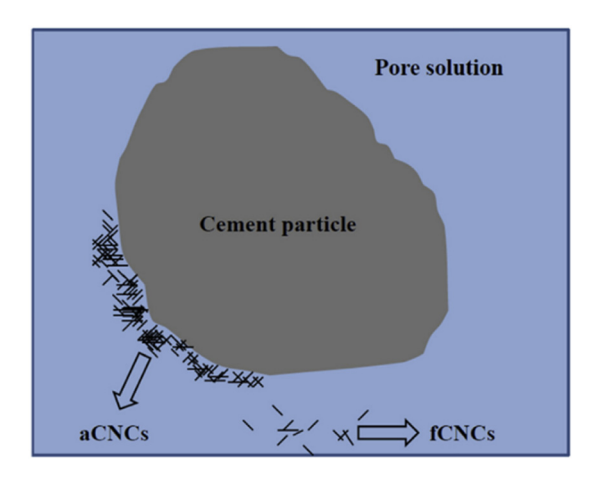


Figure 17: The schematic diagram of two different types of CNCs in the fresh cement paste, reprinted with permission from ref. [43]; Copyright 2016, Elsevier.

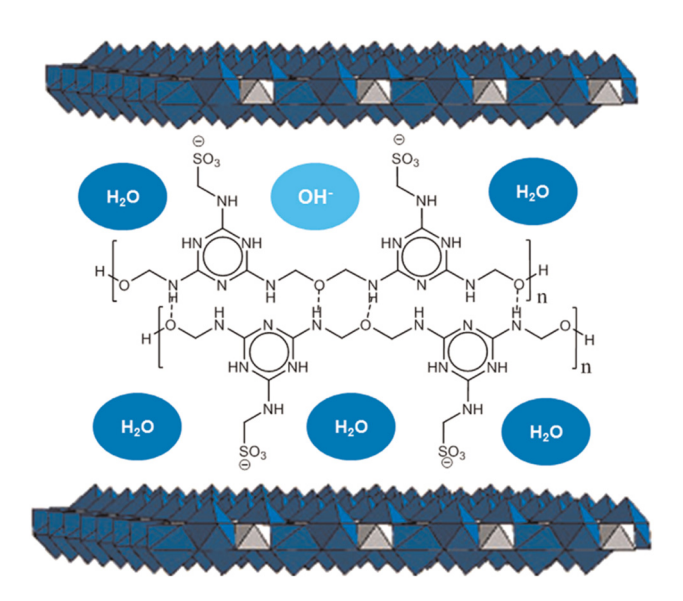


Figure 18: Schematic representation of sulfonated melamine formaldehyde intercalation compound, reprinted with permission from ref. [127]; Copyright: 2015, Elsevier.

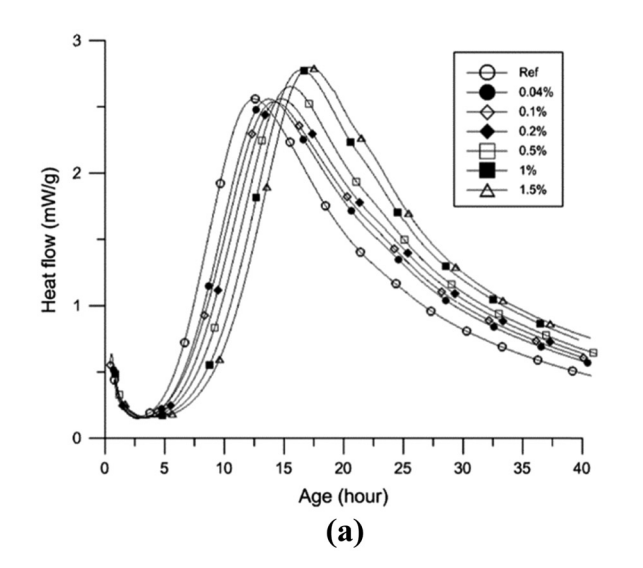
is no direct evidence showing that CNCs were intercalated in the crystalline structure of C–S–H hydration products or distorted the chemical or crystalline structure of C–S–H.

Aluminate-containing hydrates constitute an essential part (about 25 vol% in pastes) of the hydrate assemblage, which contribute to space-filling (strength development) in the same way as C–S–H and Portlandite. It was reported (as shown in Figure 18) that sulfonated melamine formaldehyde (SMF) polymers are positioned between the $(Ca_2Al(OH)_6)^+$ main sheets via electrostatic interaction

[127]. SMF can be intercalated into a hydrocalcumite host structure yielding stable (layered double hydroxide) LDH compound and the so-called inorganic–organic hybrid materials that were confirmed by XRD analysis, revealing that SMF indeed is located within the host structure [127]. There are no reports in the literature that states negatively charged sulfated cellulose nanocrystals can intercalate into $(\text{Ca}_2\text{Al}(\text{OH})_6)^+$ main sheets via electrostatic interaction. However, negatively charged sulfated cellulose nanocrystals may have good interfacial bonding with cationic cement hydrates due to electrostatic interactions.

5.2 Interactions of carboxylated (-COO⁻) CNFs with cement

Carboxylated CNFs (carboxylate content: 0.5 mmol/g-CNF) obtained by the TEMPO oxidation method have been used in cement applications. The addition of 0.3 wt% carboxylated CNFs improved the compressive strength by 50% [41]. As evidenced in Figure 19, sulfated CNCs were found to retard the hydration process [42], while the carboxylated CNF was found to accelerate the hydration process [41]. The acceleration of cement hydration at an early stage (first 24 h curing) was ascribed to the carboxylated NFC acting as nuclei to promote the formation of the hydration products. X-ray diffraction results revealed an increased volume of C–S–H products and other hydration products



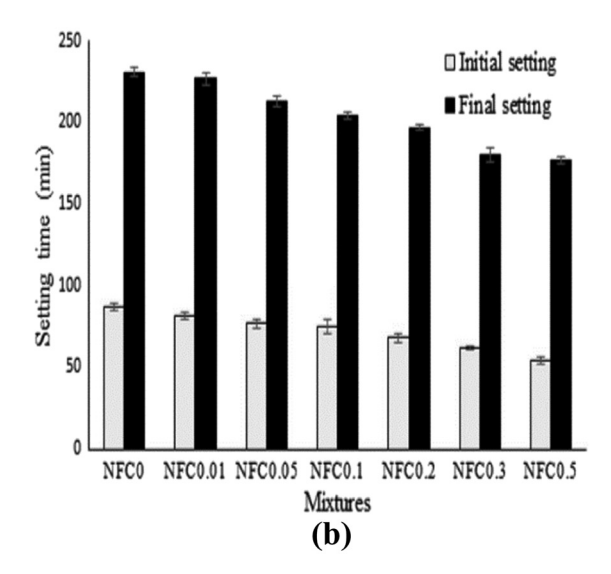


Figure 19: (a) Heat flow curves of the sulfated CNC-reinforced cement pastes for the first 40 h, reprinted with permission from ref. [42]; Copyright: Elsevier, 2015; (b) setting time of carboxylated NFC-reinforced cement pastes, reprinted with permission from ref. [41]; Copyright 2017, SAGE Publications.

such as Portlandite and ettringite. However, Jiao *et al.* [40] found that the addition of carboxylated CNFs has no clear effect on the cement hydration at an early stage, but it retarded the hydration at a later stage. As a result, the initial and final setting times were extended by about 100 and 90 mins, respectively, with the addition of 0.4 wt% of carboxylated CNFs.

Opposite cement hydration kinetics after adding carboxylated CNFs were reported in the literature by different researchers; for example, Jiao *et al.* [40] reported that carboxylated CNFs prolonged the setting time while Mejdoub *et al.* [41] observed the setting time shortened in the presence of carboxylated CNFs. Furthermore, the overall DOH was increased, and the porosity and pore size was reduced with the addition of carboxylate CNFs [40,41].

As in the previous discussion, the binding capability of carboxylate groups with metal cations, particularly Ca²⁺, was much stronger than that of sulfate groups. High surface areas and strong binding strength of Ca²⁺ with carboxylate groups make carboxylated CNFs effective nucleating agents. More hydration products are formed in the open pores which are originally filled with water, resulting in the formation of more homogeneous, dense, and compact microstructure in the presence of carboxylated NFC [40,41,120]. As a result, the interfacial bonding between carboxylated CNFs and cement hydrates can be significantly enhanced to improve the microstructure (reduced pore size and porosity) and mechanical strength of the hardened cement.

The enhanced interfacial bonding combined with high-specific surface areas of carboxylated CNFs can ensure efficient stress transfer and thus prevent the propagation of nano cracks. However, it was reported by Goncalves *et al.* [39] that the negatively charged ionic groups of CNFs could scavenge some calcium cations in the aqueous phase (as evident from the thermogravimetric analysis), which affect the formation of other hydration products, *e.g.*, ettringite and Ca(OH)₂.

As discussed, the presence of carboxylate groups will induce a series of chemical reactions around the interfaces and therefore enhance the reinforcement efficiency. Thus, CNTs have been treated by a mixture solution of sulfuric acid (H_2SO_4) and nitric acid (HNO_3) to introduce carboxylate groups on their surface. The addition of carboxylated CNTs in the cement composites exhibited improved microstructure (finer pore size distribution and reduced porosity) and enhanced mechanical properties [20], as shown in Figure 20. On the other hand, untreated carbon fibers did not improve compressive strength (Figure 20) because the bonding force between the fibers and cement matrix may be insufficient.

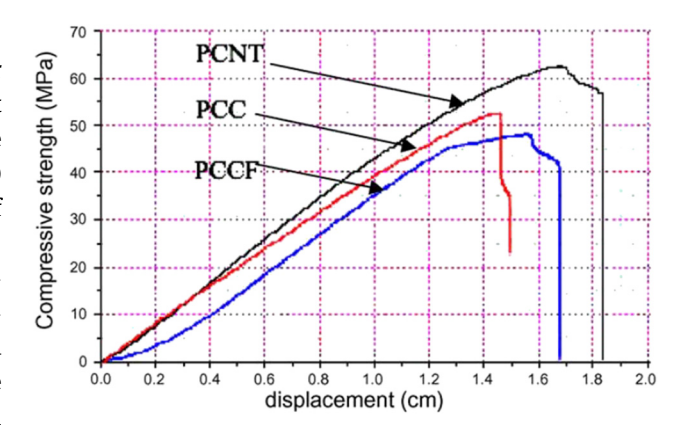


Figure 20: Typical load-displacement curves of cement-CNT composites. PCC: control Portland cement composite; PCCF: Portland cement-untreated carbon fibers composite; PCCT: Portland cement-carboxylated CNT composite, reprinted with permission from ref. [20]; Copyright 2005, Elsevier.

Based on the discussion above, we can envision the general scheme of the interfacial interaction between the carboxylate groups in CNFs and the C–S–H hydrate or Ca (OH)₂, as illustrated in Figure 21. The interaction can lead to a strong covalent bonding in the interface between the nanofibers and matrix in the composites, and therefore increases the load-transfer efficiency from cement matrix to nanofibers, and eventually results in improved mechanical strength [20,140].

There is no direct comparison of the effect of sulfate groups and carboxylate groups of PNMs on the stabilization and growth of C-S-H. However, Wang et al. [141] reported the stabilization effect of SPs with carboxylate groups or sulfate groups on the structure and properties of nano-C-S-H products. The results indicated that PCE superplasticizer is more effective for stabilization of the nano-C-S-H particles than polysulfonate (PSE) superplasticizer results in finer particle forming. This is explained by the stronger bonding between the carboxylate functional groups and C-S-H gels [141]. Moreover, XRD result indicated that PCE or PSE as stabilizers might distort the structure of C-S-H and decrease the crystallinity of C-S-H because the PCE or PSE polymers were inserted into the layer structure of C-S-H by complexation between functional groups and Ca²⁺, resulting in the interval expansion between the layers [141]. This result is consistent with that reported by Sun et al. [142], who reported that the carboxylate-metal ion groups are arranged vertically in the C-S-H layer, leading to an increase in the interlayer spacing. Sun et al. [142] also pointed out that PCE superplasticizer existed in two different locations in the C-S-H structure: grafted on the surface or partially intercalated in the interlayer regions.

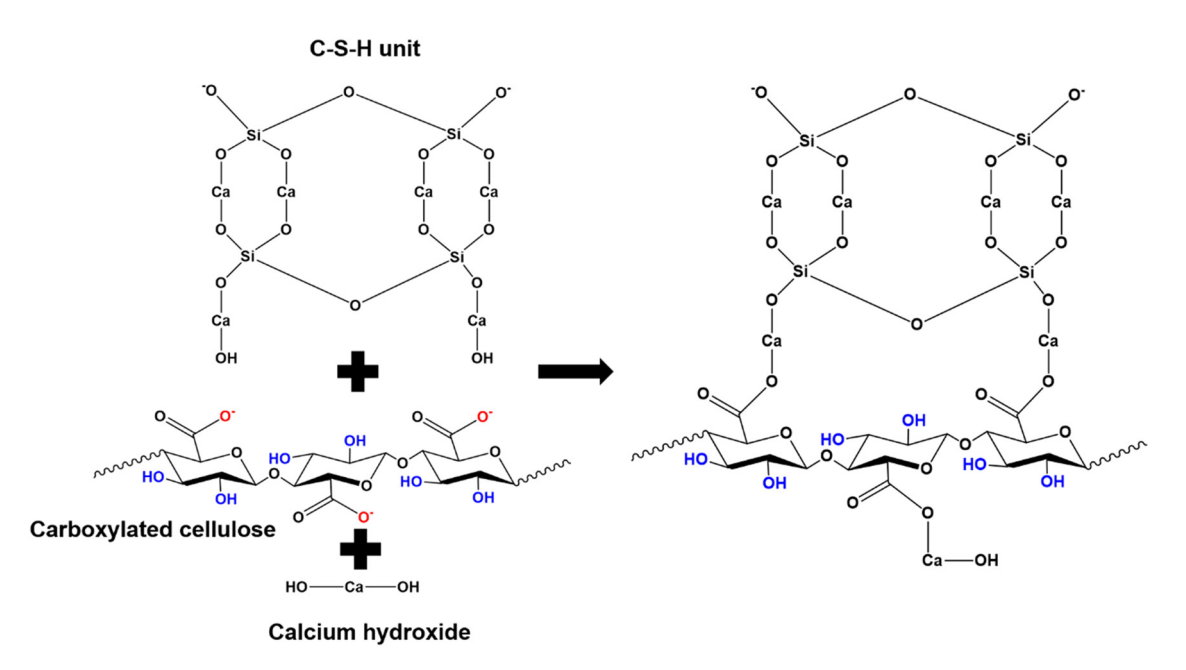


Figure 21: Reaction scheme between carboxylated CNFs and hydration products, including C-S-H and Ca(OH)₂ [20,140].

5.3 Interactions and states of mechanically fibrillated CNFs with cement

The surface chemistry on mechanically fibrillated cellulose is much simpler than those obtained by sulfuric acid hydroxide or the TEMPO-mediated oxidation method. The hydroxyl group (-OH) is the major reactive functional group on the surface of mechanical fibrillated CNFs. Carboxylate groups may exist if CNFs are mechanically fibrillated from wood pulp with a small amount of hemicellulose. Thus, some mechanically fibrillated CNFs are negatively charged [53]. Our measurements of zeta potential of mechanically fibrillated CNFs in a simulated pore solution to represent the cement pore solution about 1 h into the hydration gave a value of -51.84 ± 18.74 mV, which is a much higher absolute value than the -9.1 mV value reported for cement particles in pore solution at pH = 12.7, reported by Cao et al. [42]. Mechanically fibrillated CNFs tend to adhere to cement particles rather than agglomeration themselves. Therefore, the affinity strength between the particles have the following order: f (cement-CNF) > f (cement–cement) > f (CNF–CNF). The zeta potential results show that the affinity strength between cement and CNF is stronger than that between cement particles. Thus, mechanically fibrillated CNFs may also have an electrostatic stabilization effect on cement, thus helping improve the dispersion of cement particles. Our results show that CNCs can delay the set time of cement more efficiently than CNFs. Furthermore, the CNCs can delay the final setting time by over an hour compared to unmodified cement.

In addition, the longest delay in setting time is reached when the CNC concentration in cement is 0.05 wt% [76].

5.4 Interactions of carboxylated (-COO⁻) chitin nanofibers and nanocrystals with cement

Chitin has a similar chemical structure to cellulose, as shown in Figures 1 and 3. It can be expected that the surface chemistry of carboxylated chitin is similar to that of carboxylated cellulose. We can envision similar interfacial interactions between carboxylated chitin nanomaterials and cement. As mentioned earlier, controlling the amount of the oxidant NaClO in the TEMPO-mediated oxidation process will result in two distinct forms of carboxylated chitin nanomaterials with different amounts of carboxylate content. A low amount of oxidant NaClO can yield long and more entangled chitin nanofibers with low carboxylate content on the surface, while a high amount of oxidant NaClO can produce short rod-like chitin nanocrystals, as shown in Figure 5.

5.5 Interactions of partially deacetylated chitin nanofibers with cement

The main reactive groups on the surface of partially deacetylated chitin nanofibers are amino groups (-NH₂) and hydroxyl groups (-OH). The partially deacetylated chitin

nanofibers were stable in the acidic water medium due to the electrostatic repulsion forces induced by the protonation of amino groups. The zeta potential will dramatically drop under neutral or alkaline conditions. In our previous zeta potential measurements, the zeta potential of partially deacetylated chitin nanofibers obtained by 4 h hydrolysis by 33 wt% NaOH decreased from 44 to 16 mV when the pH was increased from 3 to 7. The absolute value of 20 mV is typically assumed to be the minimum value for moderate colloidal stability. Therefore, the partially deacetylated chitin nanofibers will tend to aggregate when increasing the pH to 7, as shown in Figure 22.

In the earlier discussions regarding the electrostatic stabilization effects of CNFs on the cement particles, the main mechanism might be that the CNFs were preferably attached to the surface of cement particles *via* electrostatic attraction. Negatively charged CNFs or nanocrystals were absorbed to the cationic surface of cement particles, thus preventing cement aggregations and improving the DOH. Our current research shows that partially deacetylated chitin nanofibers have a positive surface charge under acidic and alkaline conditions.

Hall [98] reported that chitin nanocrystal with amino functional groups ($-NH_2$) or amide groups (-NHR) was ideal to be used as a corrosion inhibitor in the cement because they can form strong films on the surface of metals through non-covalent binding with the metal surfaces. Whether the partially deacetylated chitin nanofibers or mechanically fibrillated chitin nanofibers have a similar corrosion-inhibiting behavior is yet to be proven in future work.

5.6 Interactions of mechanically fibrillated chitin nanofibers with cement

The reactive hydroxyl group (-OH) is the primary functional group on the surface of mechanically fibrillated

chitin nanofibers. There are a small number of amino groups on the surface of chitin nanofibers due to a small fraction of deacetylation during the extraction process, as mentioned previously. Suspensions of mechanically fibrillated chitin nanofiber were unstable in the neutral or alkaline condition but did not show any issues dispersing in the alkaline cement pore solution. With their surface charges, we found that chitin nanofibers at a concentration of 0.035 wt% delay the initial and final setting times of cement paste by 35 and 78 min, respectively. Lower or higher concentrations attain shorter setting times. Higher electrostatic repulsion of chitin nanofibers due to high zeta potential values ($-28.04 \pm 2.6 \,\mathrm{mV}$ in simulated pore solution) and high density of functional groups might be the contributing factor for the nanochitin function as a set retarder.

Typically, the addition of nanoparticles accelerates cement hydration because small particles might provide more heterogeneous nucleation sites and/or space where hydration products can grow [107,143]. Nucleation sites of nanoparticles will promote a more homogeneous,

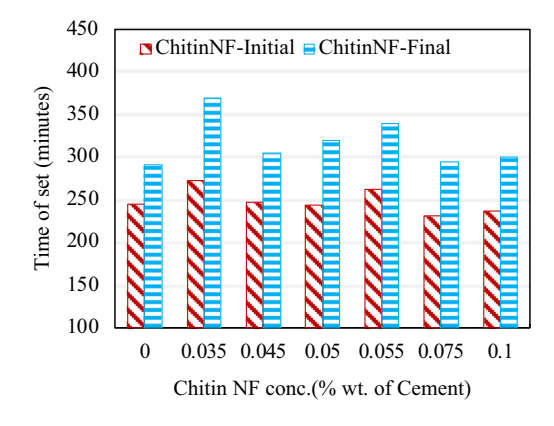


Figure 23: Effect of concentration of chitin nanofibers on the setting time of cement paste.

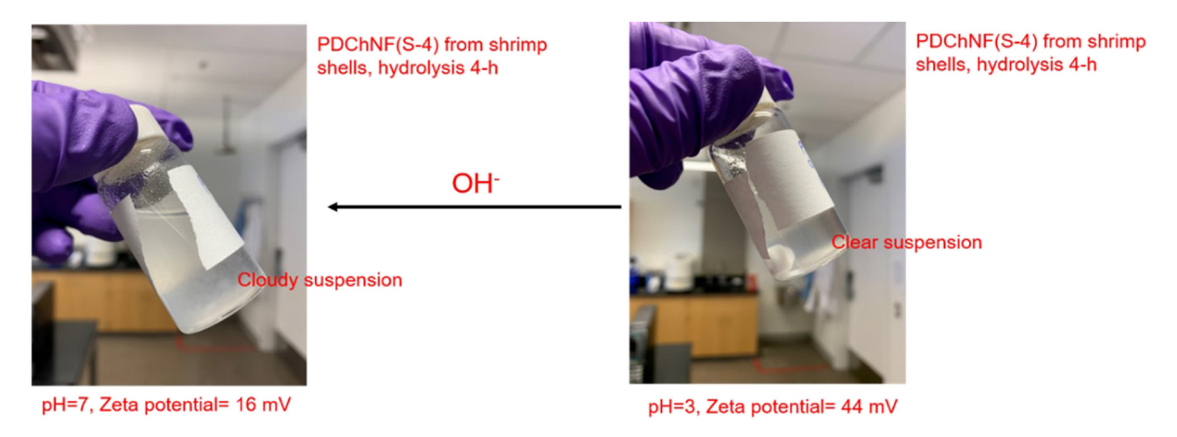


Figure 22: Partially deacetylated chitin nanofibers in acidic or neutral media.

denser cement microstructure. This is attributed to the filling effect, which can enhance hydration product growth in the pore space and filling voids between the cement (clicker) particles, and hence a reduction in porosity, as shown in Figure 23. PNMs can act as heterogeneous nucleation sites and thereby accelerate the formation of C-S-H nuclei. Peschard et al. also reported that polysaccharides could restrict the C₃A hydration rather than promote nucleation [69]. More work is still needed to elucidate the combined effect of the nano-size effect and ionic absorption capability of PNMs on the phase composition chemical and crystalline growth of hydration products.

6 Strength-enhancing mechanisms of PNMs in cement composites

Polysaccharide-based materials could have a significant effect on the mechanical performance of cement composites. Previous studies regarding the effect of PNM type, source material, production method, size, and surface functional groups on the mechanical properties of cement composites, as well as the mechanical properties, were summarized in Tables 1 and 2. Table 3 includes a summary of studies of cement using PNMs and also other derivatives of chitin and chitosan. The effect of PNMs on properties other than strength, such as setting time and rheology, is also listed in these tables wherever available.

A consensus from Tables 1 and 2 is that CNFs and CNCs can increase the compressive and/or flexural strength at different dosages, though contradicting findings were reported in some cases. For example, several studies [34,37,40,144] reported a flexural strength increase from 15 to 72% using CNFs and Jiao et al. and Mejdoub et al. [40,41] reported a 20–43% increase in compressive strength using CNFs. In contrast, Hisseine et al. and Rosato et al. [36,145] reported a reduction in the compressive strength of cement in the presence of CNFs. However, the reason was not explained. For CNCs, Cao, Dousti, and Mazlan et al. [42,45,46] reported increased flexural strength.

Generally, four possible mechanisms are proposed for elucidating the improved mechanical performances of cement by PNMs addition: (1) bridging/reinforcing effect; (2) filling effect, with high modulus PNMs increase the overall modulus of the composite; (3) more nucleation sites due to high surface area; (4) internal curing by releasing adsorbed water to increase the DOH. A detailed discussion of these mechanisms, as seen in the various literature gathered in Tables 1, 3, is provided following

the tables. In addition, the effect of properties of PNMs listed in Tables 1–3, i.e., size, aspect ratio, production method, dispersion, concentration, etc., are also discussed following the tables. In Tables 1–3, fs stands for the flexural strength, and Cs is the compressive strength. The letter d is the abbreviation of day. E is Young's modulus.

6.1 Bridging effect

The bridging effect of nanofibers in the cement composites matrix has been considered as one of the reinforcing mechanisms for the mechanical improvement because the bridging effect in the matrix can provide sufficient load transfer from the matrix to the nanofibers and delay the propagation of nano-cracks and restrain nano-cracks [146]. Much more energy is needed to break the crack bridging by the nanofibers than that for the crack growth of cement matrix, thus leading to improvement in the flexural and compressive strengths of cement [146,147]. The fracture energy was a measure of crack initiation and growth through cementitious materials [148]. With the bridging effect of nanomaterials, more energy is needed to break the crack bridging of nanomaterials. It was reported that the addition of CNFs at a concentration of 0.15% could significantly increase fracture energy of cement by 60%, suggesting that CNFs are effective in preventing crack growth and thus the flexural strength was also increased by 116% [37]. It was also reported that the addition of TOCNFs (carboxylate content: 1.1 mmol/g fiber) could result in a decrease in the average cracking area by about 23% at 0.8 wt% CNF [38]. The bridging effect of cellulose nanomaterials in the polymer matrix has also been considered as a significant factor contributing to the improvement in polymer nanocomposites. The potential scheme of fracture mechanism was also proposed by Xu et al. [149], as shown in Figure 24a. It was reported that at the same nanocellulose concentration, the bridging effect of CNFs in the polyethylene oxide (PEO) matrix was more pronounced than that of CNCs. Thus, CNFs led to higher strength and modulus because of a larger aspect ratio of CNFs and fiber entanglement. To our knowledge, the bridging mechanism of cellulose nanomaterials in the cement matrix is still rarely reported in the literature and has not been fully elucidated [77,150]. Our study recently submitted for peer-review shows that chitin nanofibers and nanocrystals can increase the compressive strength of cement paste by up to 12% and flexural strength by up to 41.4% (Haider et al., [103]).

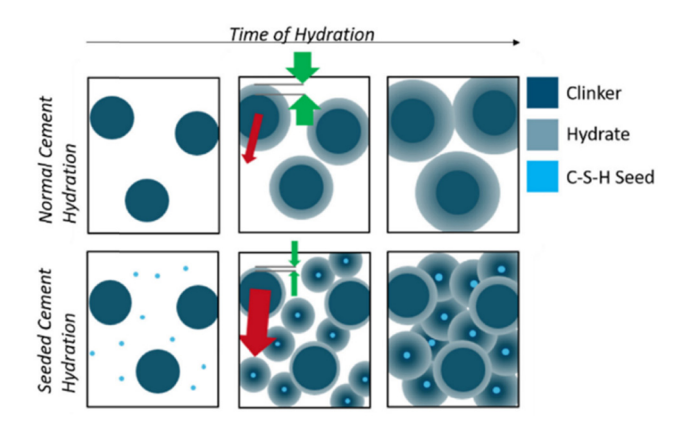


Figure 24: Schematic representation of cement hydration and the influence of nucleation seeding with C-S-H. The red arrows display concentration gradients, while the green arrows highlight the different thicknesses of the hydrate formed around the clinker particles, reprinted with permission from ref. [105]; Copyright 2018, Elsevier.

As for CNFs-reinforced cementitious materials, the potential scheme of the bridging between CNFs and hydration products is depicted in Figure 25b [34]. Figure 25c shows a typical "pull-out mechanism" of the low weight fraction of CNFs (0.04 wt%) in OWC composite, the authors mainly attributed about 20% increase in the flexural strength to such bridging effect of CNFs in OWC matrix and well dispersion of CNFs at low dosage (0.04 wt%) [34].

6.2 Filling effect and increased hydration for porosity reduction

Research has shown that with the aid of cellulose nanomaterials, the DOH of cement can be enhanced and the porosity can be reduced. Thus, the mechanical performance of cement can be improved. It was reported that the addition of CNCs was beneficial for cement particles reacting more efficiently with water, thus leading to increased DOH and flexural strength [42]. Two mechanisms were proposed to explain CNCs' contribution to increased DOH. One is the steric stabilization effect of CNCs, by which cement particles are well separated. This mechanism was also supported by the results reported by Flores et al. [78]. The other is a short-circuit-diffusion (SCD) effect suggested by Cao et al. [42] as schematically depicted in Figure 26. One possible scenario is that when CNCs absorb on cement particles and remain in the hydration shells (hydration products), a path will form and help transport water transportation from capillary pores to the inner unhydrated cement cores. This may facilitate a significantly increased fraction of cement reacting with water compared with the cement pastes without CNCs [42,151]. The outcome of increased DOH with adding CNCs is the reduction in total porosity of cement, thus leading to improved mechanical properties [151]. Onuaguluchi et al. [33] also reported that the addition of CNFs could increase the DOH, thus improving strength. Haddad Kolour [37] also proposed a similar "Tunnel" mechanism similar to the SCD mechanism proposed by Cao et al. [42]. According to Haddad Kolour [37], at the hydration acceleration stage, adhered CNFs will be covered by LD C-S-H (outer-products). While at the hydration deceleration stage, when the surface is completely covered by LD C-S-H, HD C-S-H growth starts within the cement particles. The porous space around these adhered CNFs will work as "Tunnels" for transporting water to unhydrated cement grain, which in turn help to produce more HD C-S-H (inner-product) and enhance total hydration reaction. Around 8% hydration improvement [37] was observed in the presence of CNFs. It should be mentioned that though these theories attempt to explain the increase in DOH induced by CNC and CNF additions, they are yet to be experimentally proved at the molecular level and thus remain as working hypotheses.

6.3 Increased modulus of C-S-H and increased HD C-S-H fraction and influence of nucleation sites

The improved mechanical properties of nanocellulosereinforced cement may also be attributed to the increased modulus of C-S-H and an increased portion of HD C-S-H. It was reported that the CNC addition could significantly increase the modulus of HD C-S-H [42]. The HD C-S-H fraction was also increased by the CNC addition, as shown in Figure 27 [78]. There are three possible reasons for the increased modulus of HD C-S-H: (1) the incorporation of high-modulus CNC in C-S-H, crystalline cellulose has an elastic modulus in the axial direction of 110-220 GPa [30]; (2) the CNC incorporation can modify the C-S-H structure and chemistry [151]; (3) CNC can act as a nucleating agent to promote the formation of C-S-H crystals. As mentioned earlier, the role of cellulose nanomaterials as a nucleating agent for the crystallization of polymer in polymer composites has been extensively reported and demonstrated in the literature [40,41,120]. As a result, the nucleating agent cellulose nanomaterials can increase the degree of crystallinity of the polymer matrix. The enhanced crystallinity contributed to the improvement in the stiffness of the composite materials, which is difficult to dissociate from the real direct

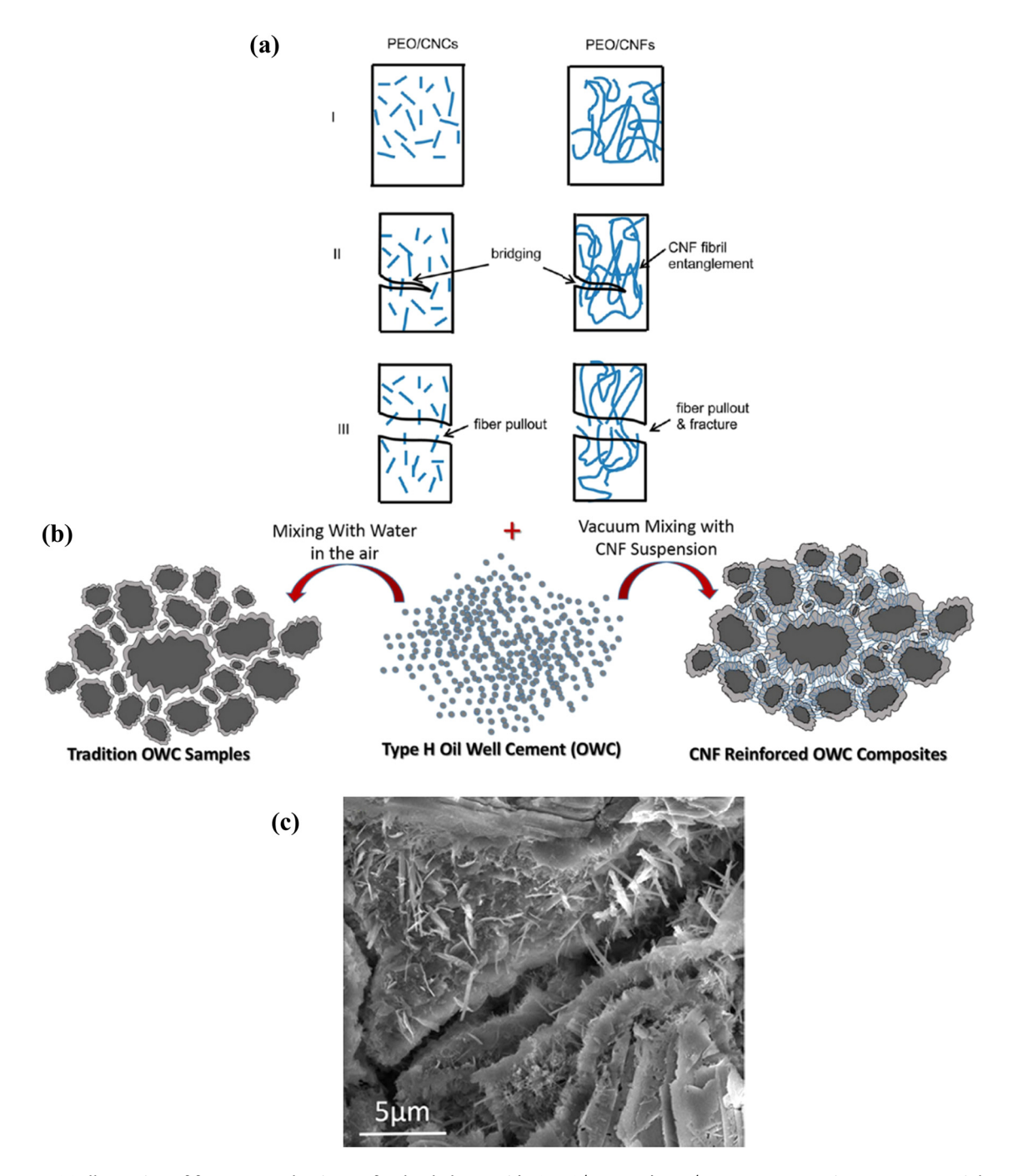


Figure 25: (a) Illustration of fracture mechanisms of polyethylene oxide (PEO)/CNC and PEO/CNF nanocomposites [149]; Copyright 2013, American Chemical Society; (b) scheme of CNF reinforced oil well cement composites; (c) SEM image of CNF reinforced OWC composites with 0.04 wt% CNF loading [34]; Copyright 2016, Nature Portfolio.

reinforcing effect of the nanoparticles [48,53]. Hydrophilic nature and high specific areas of PNMs may also act as nuclei sites to promote the nucleation of the crystals of C–S–H hydration products, thus leading to the formation of a more compact, denser, and stronger structure than the mixture without nanocellulose [41,78,117]. However, this nucleating effect of cellulose nanomaterials has not been

experimentally demonstrated yet. There is also a contradictory view [40] on the role of CNFs as nucleating sites in facilitating the growth of crystalline hydration products. It says that the oxygen atom in the hydroxyl and carboxyl group has unpaired electrons, which can react with calcium ions and form a hydrophilic complex that can adsorb on cement particles. Thus, the number of active sites

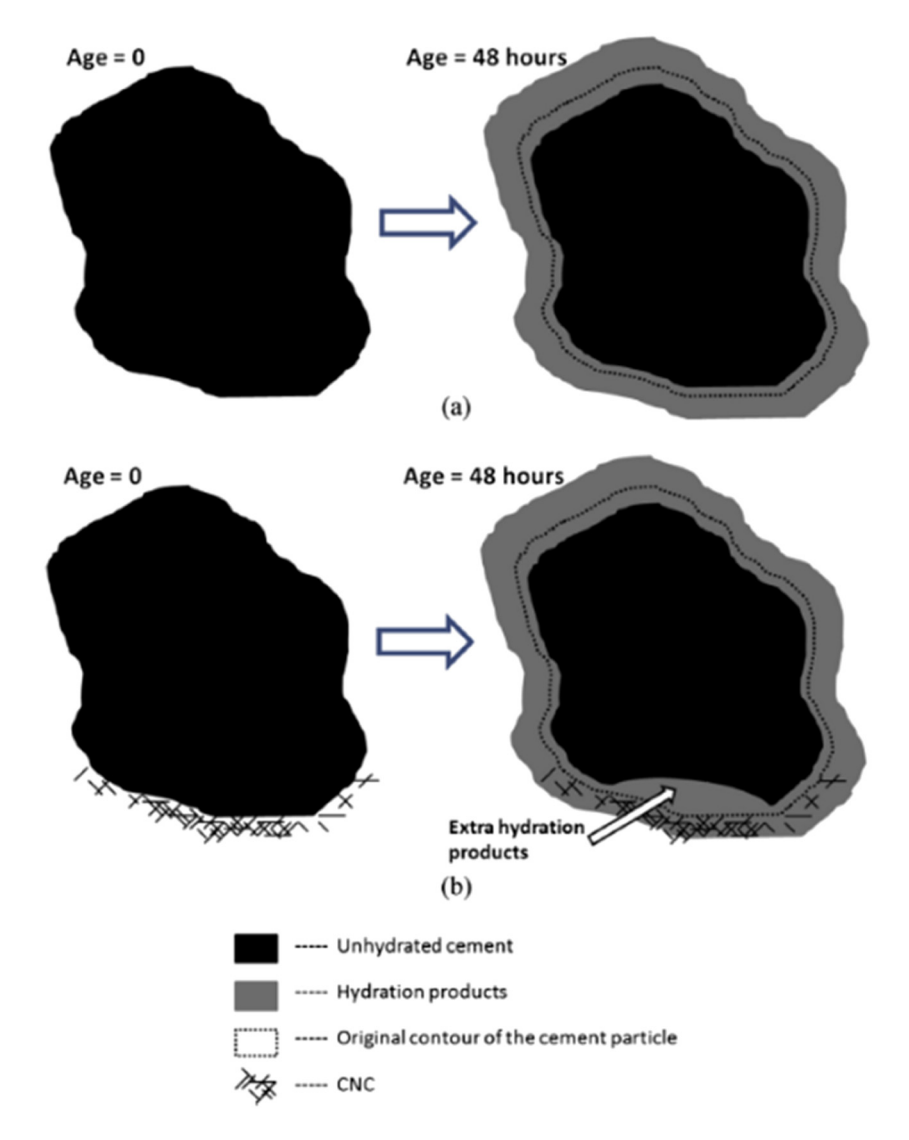


Figure 26: A schematics illustration of the proposed hydration products forming around the cement grain from the age of 0–48 h in the (a) plain cement and (b) cement with CNCs on a portion of the cement particle showing short-circuit-diffusion mechanism [42]; Copyright 2015, Elsevier Ltd.

between cement particles and water decreases, and the distances between cement particles increase. The adsorption and complexation effects reduce the surface activity of the hydration products and retard the production of calcium hydroxide crystals, thus the cement particles with higher addition of CNFs took a longer time to hydrate [40].

6.4 Internal curing agent

Generally, the early-stage autogenous shrinkage of cement occurs within the first 24 h after mixing with water. And the cement matrix is more prone to cracking during the first 12 h of hydration. During this period, the tensile strength of cementitious materials is too low to prevent

the crack propagation induced by shrinkage stresses. CNCs can retard the hydration at an early stage because the majority of CNCs (>94%) adhered to the cement particles and reduced the reaction surface area between cement and water [42]. As shown in Figure 19, CNCs decreased the initial hydration rate, but the overall DOH increased with CNCs addition. Figure 19a shows the heat flow curves for the seven CNCs–cement pastes, while Figure 27 shows the cumulative heat flow curves during the first 40 h, from which it can be observed that the heat flow is delayed with increasing CNC concentrations. For instance, the heat flow peak is reached at 12 h for the reference mixture (0%), while the peak is reached at around 17 h for the mixture with 1.5% CNCs. The retardation of the peak heat flow could indicate CNCs adhering to the cement particles and,

2702 — Tuhua Zhong et al. DE GRUYTER

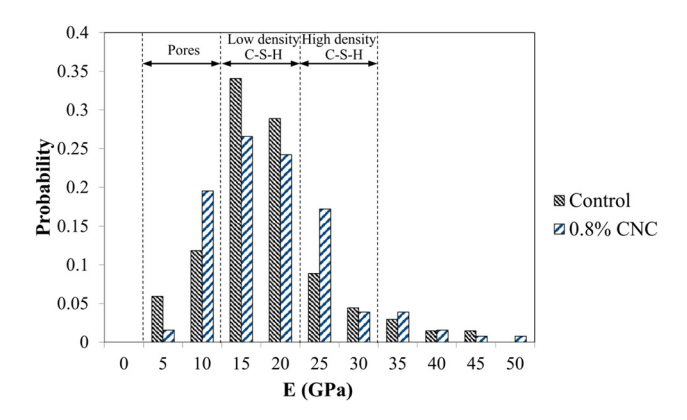


Figure 27: Nanoindentation results showing the probability distribution of Young's modulus of CNC-reinforced cement corresponding to 28 days of curing, reprinted with permission from ref. [78]; Copyright 2017, MDPI.

therefore, blocking the cement particles from reacting with water at an early age. At the early stage, the slowing down of the hydration can help prevent the destabilization of the matrix by preventing fast water loss as cement hydration proceeds. CNFs also exhibited the same retardation effect of cement hydration at an early stage [33]. However, Mejdoub *et al.* [41] observed that carboxylated CNFs in cement paste accelerate the early hydration. In fact, after 1 day of curing, the DOH increases by 1.6%, 19.3%, 32.6%, 66.0%, 87.3%, and 102% for the mixture containing 0.01, 0.05, 0.1, 0.2, 0.3, and 0.5 wt% CNFs, respectively. The authors ascribed the acceleration of cement hydration at an early stage to the nuclei effect of CNFs.

In addition, CNFs have a high water retention capacity [38]. Haddad Kolour [37] suggested that CNFs can act as a "reservoir" like superabsorbent polymer because CNFs are hydrophilic and can retain some water. This stored water can be released later and work as a supplementary source of water, thus reducing autogenous shrinkage. Adding 0.06 and 0.09% CNFs can reduce autogenous shrinkage up to 49 and 26%, respectively, as shown in Figure 28. Thus, CNFs can work as an internal curing aid to prevent autogenous shrinkage in cementitious materials because water absorbed by CNFs migrates to the cement pastes and provides internal water for unhydrated cement particles, thus offering a decent internal curing environment during the hardening process of cement paste [33,117]. TEMPO-mediated oxidation pretreatment can introduce the hydrophilic carboxylate groups to the surface of CNFs, thus further increasing the water retention capacity. Therefore, CNFs with carboxylate groups resulted in better flow control of the wet cement paste and reduced the crack growth in concrete [37] (Figure 29).

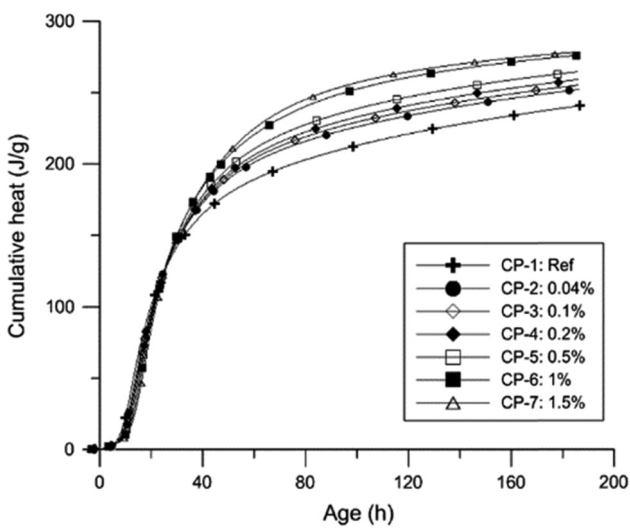


Figure 28: Cumulative heat flow curves of the cellulose nanocrystal-cement pastes at different CNC concentrations, reprinted with permission from ref. [42]; Copyright 2015, Elsevier. Note: Figure 19a in Section 3.5 shows the heat flow curves.

7 Impact of other properties of PNMs on cement properties

7.1 Size and morphology

Based on the distinctive size and morphology, PNMs can be categorized into nanofibers and nanocrystals. As shown in Figure 30, nanofibers usually have a complex, highly entangled web-like structure and usually have a large aspect ratio (4–20 nm in width and 500–2,000 nm in length). Nanocrystals often have a needle-like or rod-like structure with a low aspect ratio (less than 10 nm in width, 50–500 nm in length) [30,48]. By controlling the TEMPO-mediated oxidation parameters, *i.e.*, the amount of oxidant NaClO, two different chitin nanomaterials (chitin nanofibers and chitin nanocrystals) were obtained in our current research, as shown in Figure 6.

The smaller size of PNMs leads to a higher specific area, thus favoring the effective interaction with the matrix to ensure the load transfer from the matrix to the reinforcement [41,144]. It was reported that the addition of 3.3 wt% NFC in the cement mortar improved the flexural strength and the modulus of elasticity by 26.4 and 41.5%, respectively, in comparison to cement mortar reinforced with the sisal fibers [144]. A high aspect ratio of nanocellulose may be more effective in stabilizing crack tips, thus suppressing cracks [148]. Many claims are based on the fact that long fibers can help delay crack propagation or even lead to crack arrest. While the length

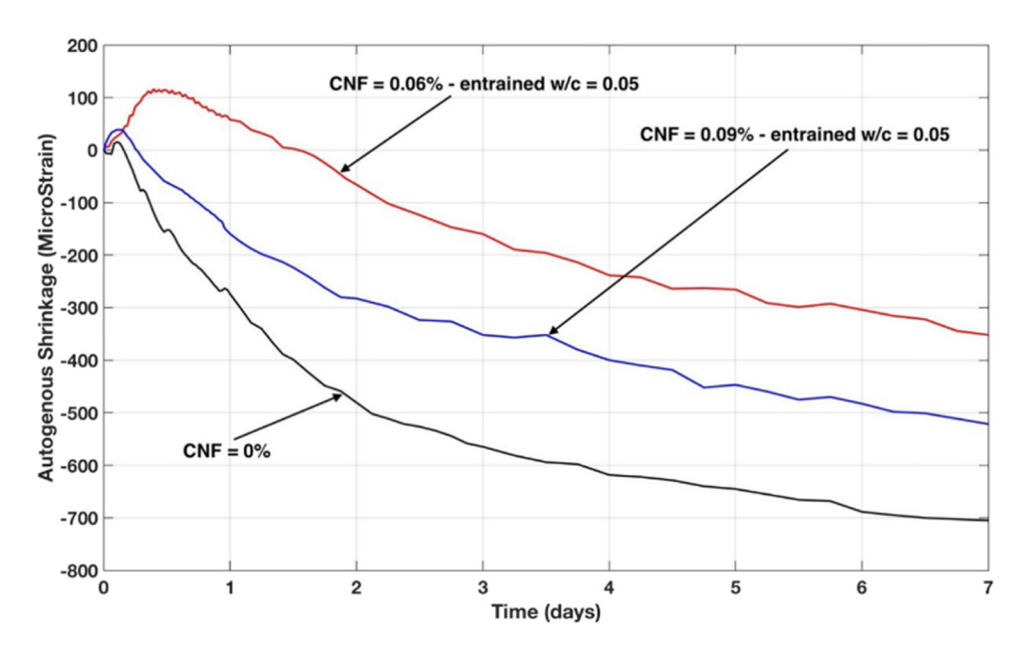
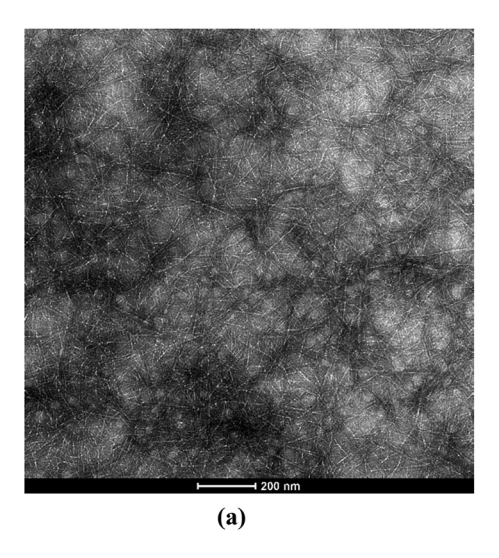


Figure 29: Autogenous shrinkage of cellulose nanofibrils-reinforced cement pastes as a function of time, reprinted with permission from ref. [37]; Copyright 2019, The University of Maine.

of CNCs is much smaller than CNFs, its ability to reinforce the cement needs to be further examined [146]. In addition, systematic studies are required for understanding the effects of nanofibers and nanocrystals on the mechanical performances of cementitious materials.

7.2 Concentration

A high concentration of nanomaterials in the cement paste increases the chances of agglomeration, which can be detrimental to the mechanical properties of cement composite materials. The optimal nanocellulose concentration for improving cement mechanical properties may vary depending on the type of nanocellulose, the sources for nanocellulose production, the way of adding the nanocellulose, the degree of dispersion, the type of cement, water-to-cement ratio, use of water reducer admixtures, *etc.* Onuaguluchi *et al.* [33] evaluated cement pastes by incorporating CNFs from bleached pine pulp at levels of 0.05t%, 0.1, 0.2, and 0.4 wt%. The results showed that the pastes reinforced with 0.1% nanofibers showed an increase of 106% in flexural strength and 184% in energy absorption, compared to pastes without nanofibers. High



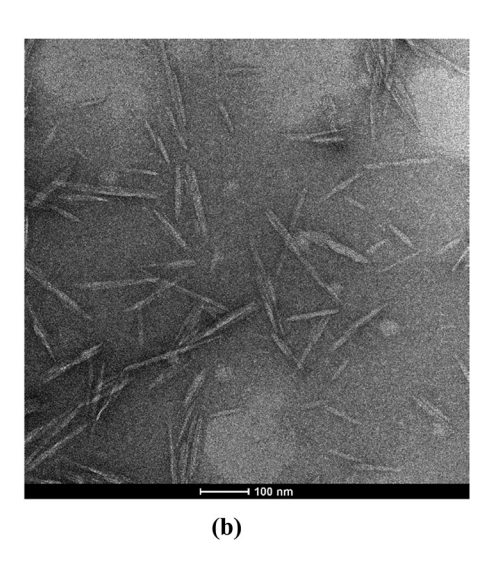


Figure 30: (a) TEMPO-oxidized CNFs and (b) CNCs prepared by acid hydrolysis.

concentration of CNFs (above 0.1 wt%) resulted in a decrease in flexural strength which likely results from CNF agglomerates observed through SEM analysis.

Our results show a 17-18% increase in the compressive strength in the presence of CNFs or CNCs in comparison with the control samples. The maximum strength is reached at a concentration of 0.065 wt% for CNFs and 0.4 wt% for CNCs and after these concentrations, the strength declines. Haddad Kolour et al. [37] reported that adding 0.15% cellulose nanofibrils in the cement pastes could improve flexural strength and fracture energy by 116 and 60%, respectively. Mejdoub et al. [41] used TOCNF and found that maximum compressive strength was achieved in the presence of 0.3 wt% TOCNF. When the concentration of TOCNF is above 0.3 wt%, the strength decreased. It was explained [41] that TOCNF aggregates created weak zones in the form of pores which cause stress concentration in the cementitious matrix and promote premature cracking. The microcracks were found in the presence of 0.5 wt% TOCNF.

7.3 Dispersion

The degree of dispersion of nanomaterials in the matrix is one of the most critical factors governing the reinforcement effects of cement mechanical properties. The agglomerates of PNM in the matrix may act as defects or stress concentrators, which is detrimental to the mechanical properties of the cement. Cao *et al.* [151] reported that effective dispersion of CNCs to reduce agglomerates could be achieved by tip

ultrasonication. As a result, the DOH of the cement could be increased. Flexural strength was also increased by up to 50% for cement paste containing sonicated CNCs compared to the 20-30% increase for the cement pastes containing raw and not sonicated CNCs at 0.2 vol% CNC concentration. Cao et al. [43] also found that CNCs preferred to attach to cement particles without sonication, while they are more randomly dispersed into the matrix after sonication. However, there are no obvious changes in SCD with and without sonification. Haider et al. [76,103] found that ultrasonication seems to have a positive effect on the light transmission of CNC suspensions, as shown in Figure 31. The three figures show that with longer durations of sonication time, suspensions with higher contents of CNCs (0.10 and 0.15 wt%) provide higher transmission of light due to a more uniform dispersion. On the other hand, the mechanically fibrillated CNF suspensions allowed negligible (<5%) light transmission during UV-Vis spectroscopy due to their weblike and entangled morphology. The morphology of the two types of chitin nanomaterials before and after 30 min sonication is shown in representative micrographs in Figure 32. As shown in Figure 32a and b, CNFs displayed an entangled network-like morphology with elongated, interconnected fibrils.

CNCs agglomerates may bring air entrapment, which will cause an increase in the porosity. In addition, CNCs agglomerates absorb water, and unreacted water may form the capillary pores [43]. The pore size distribution study shows that sonication [43] helps reduce the porosity due to less formation of large size capillary pores. This may attribute to the fact that sonification can break the CNC agglomerates and result in better dispersion.

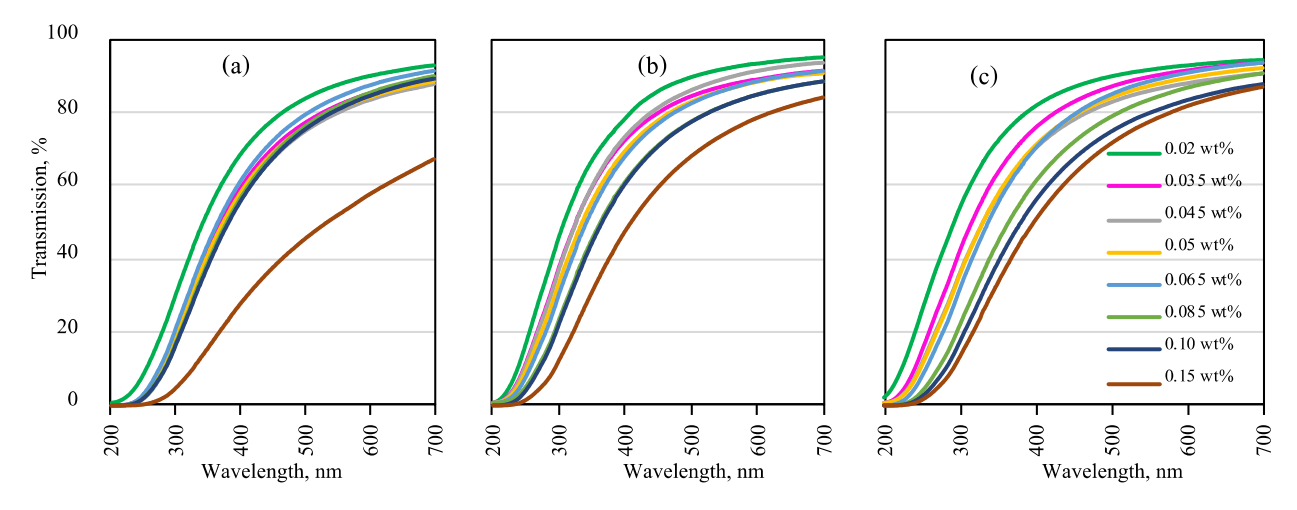


Figure 31: Effect of sonication on the dispersion of CNCs in DI water based on UV-Vis spectroscopy after (a) 2 min, (b) 10 min, (c) and 30 min sonication, reprinted with permission from ref. [76]; Copyright 2021, Elsevier Ltd.

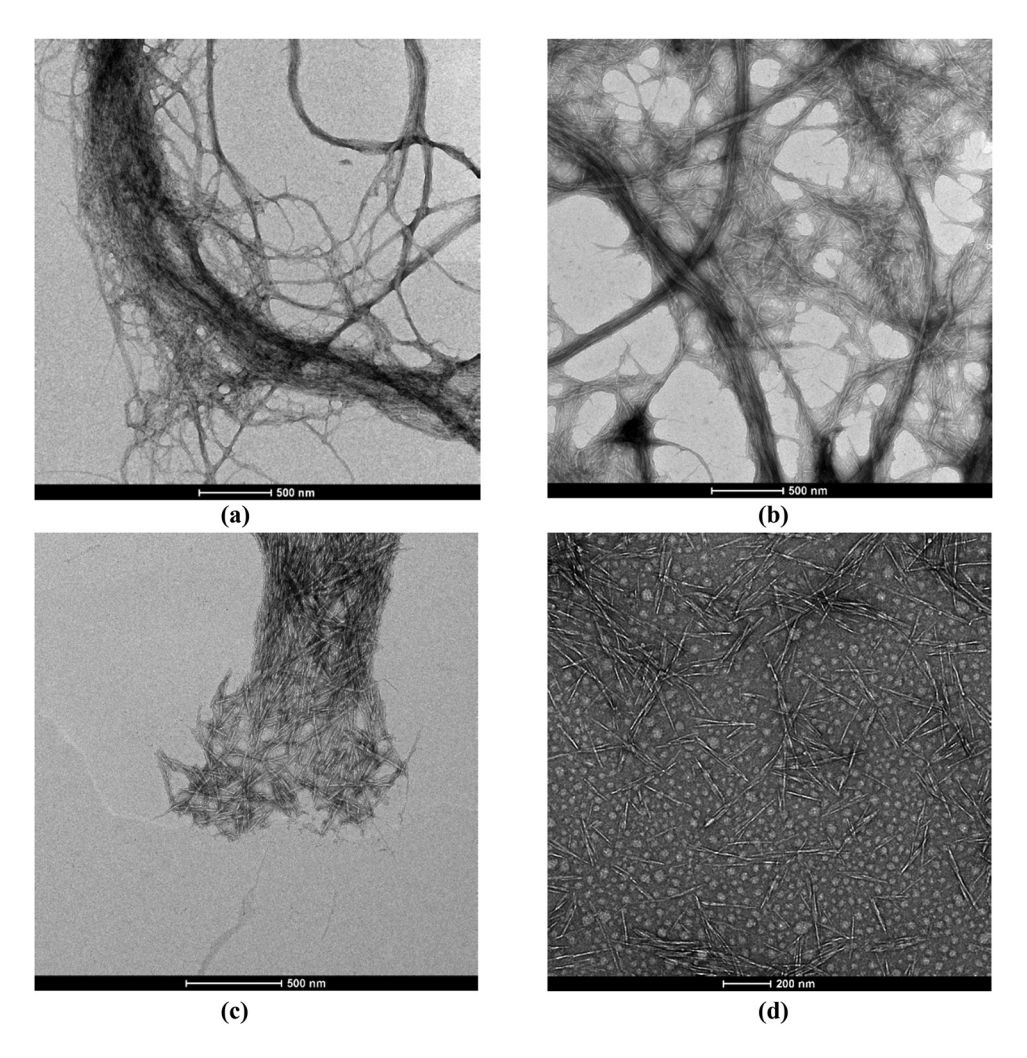


Figure 32: Morphology of CNFs: (a) before sonication and (b) after 30 min sonication; the morphology of CNCs: (c) before sonication and (d) after 30 min sonication, reprinted with permission from ref. [76]; Copyright 2021, Elsevier Ltd.

7.4 Surface chemistry

The surface chemistry of nanocellulose is mainly determined by the manufacturing or extraction methods. CNCs are usually isolated from semi-crystalline cellulose fibers using a traditional strong acid hydrolysis process in which the amorphous region is digested. The left intact crystallites are then released with the assistance of mechanical disintegration processes (e.g., ultrasonication) [48]. Sulfuric acid is one of the most used inorganic acids for introducing anionic sulfate half-ester groups on the surface of crystallites through the reaction with the hydroxyl groups. These negatively charged functional groups play important roles in stabilizing CNCs in water [48]. CNFs can be extracted through TEMPO-mediated oxidation pretreatment followed by mechanical disintegration. The TEMPOmediated oxidation method is regarded as an effective and efficient way to produce CNFs because primary hydroxyl

groups are selectively converted into anionic carboxylate groups (-COO⁻) under alkaline conditions. The negative charges induce interfibrillar electrostatic repulsion forces and thereby facilitate nanofibrillation in the subsequent mechanical separation process [54,55]. The remarkable advantage of sulfuric acid hydrolysis and the TEMPO-mediated oxidation method is that both methods can introduce negatively charged groups on the nanocellulose surface and promote the formation of stable sulfated CNCs and TOCNFs in water due to interfibrillar electrostatic repulsion forces.

Good dispersion of cellulose nanomaterials in water is a prerequisite to ensure their reinforcing effects when applied to cementitious materials. It was reported by Cao *et al.* [42] that cement particles have a high tendency to aggregate because cement particles have a zeta potential of about –10 mV compared to –64 mV for sulfated CNCs. The addition of negatively charged CNCs helps the

dispersion of cement particles and prevents aggregation due to the steric stabilization effect of CNC, thus leading to the increased overall DOH of cement. Negatively charged TOCNFs, TOChNFs, or TEMPO-oxidized chitin nanocrystals (TOChNCs) may have the same electrostatic stabilization effects for cement particles in water, although few reports are found in the literature. As discussed previously, cellulose nanomaterials may work as an internal curing aid to prevent autogenous shrinkage and early crack propagation in cementitious materials with the release of water retained by cellulose nanomaterials [33,117]. Carboxylated CNFs have a higher water retention capacity. When the density of carboxylate groups on the cellulose surface increases from 0.13 to 1.44 mmol/g fiber, the water retention value increases from 3.62 to 13. 4 g/g fiber. Carboxylate-rich CNFs with high water retention value are a better internal curing aid to prevent autogenous shrinkage [38]. The introduction of carboxylate groups (-COO⁻) can be readily achieved by the TEMPO-mediated oxidation method and the carboxylate content can be conveniently controlled by the oxidation conditions [54,55]. Mejdoub et al. [41] found that TOCNFs could reduce the cement porosity by 36% and increase the compressive strength of cement by 46%. The authors have attributed the improvement to the potential chemical interactions between the carboxylate groups of the TOCNFs and C-S-H hydration products because this reaction can increase a strong interfacial bonding between the reinforcement and the matrix, thus facilitating an effective stress transfer from the matrix to the reinforcement. However, the details of how carboxylate groups on the surface of cellulose nanomaterials react with the components in the cement are not elucidated.

The introduction of carboxylate groups to the surface of CNTs can improve its dispersion in water and enhance the interfacial interaction between carboxylated CNTs and the cement matrix. CNTs can be modified by concentrated sulfuric acid (H₂SO₄) and nitric acid (HNO₃). Nanocomposites with carboxylate-functionalized CNTs [20] clearly showed higher strength than those with pure CNTs. And the treated CNTs were found to be tightly wrapped by C-S-H, indicating interfacial interaction between CNTs and the hydration products (e.g., C-S-H and calcium hydroxide). The strong interfacial interaction between CNTs and the hydration products produces a high bonding strength between the reinforcement and the cement matrix, as schematically depicted in Figure 33 [20]. The interaction leads to a strong covalent force on the interface between the reinforcement and matrix in the composites and therefore increases the load-transfer efficiency from the cement matrix to nanotubes. As a result, the

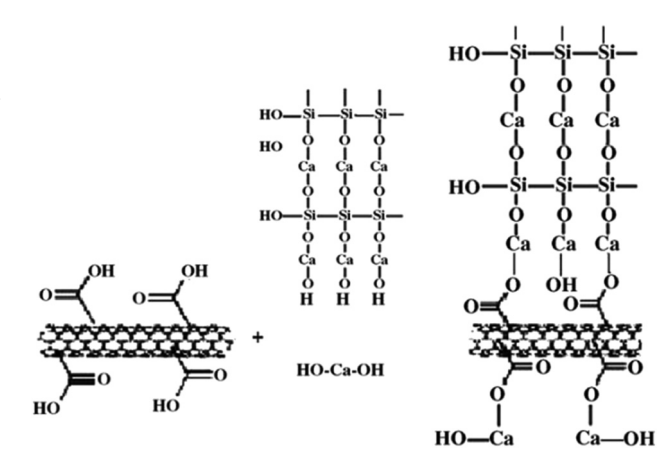


Figure 33: Reaction scheme between the carboxylated nanotubes and hydrated production (Ca(OH)₂ and C-S-H) of cement, reprinted with permission from ref. [20]; Copyright 2005, Elsevier Ltd.

mechanical properties of the composites are improved. Carboxylated CNTs were also found effective in reducing the porosity in the cement composites which is likely due to high strong interfacial bonding between carboxylated CNTs and the cement matrix. As the porosity of the composites is reduced, the strength of composites increases [20].

Calcium ions (Ca²⁺) can form CaOH⁺ complexes in an aqueous solution (Wang et al.). In addition, carboxylate groups are functional chelating groups that can absorb metal ions (Palacios et al.). Carboxylate groups on the surface of CNFs thus can chelate with calcium ions and absorb on cement particles via electrostatic attraction, which can act as nucleation sites and form interfacial bonds and produce mechanical interlocking between the reinforcement and the matrix [41,152]. TEMPO-mediated oxidation method has also been used to extract chitin nanomaterials in our study [103]. As shown in Figure 34, negatively charged carboxylate groups can not only induce interfibrillar electrostatic repulsion forces for stable dispersion, but also can improve the interfacial interaction between carboxylated chitin nanomaterials and the cementitious materials. Therefore, carboxylated chitin nanomaterials may be a promising nano-reinforcement alternative to CNTs and cellulose nanomaterials for cementitious materials.

As shown in Tables 1–3, polysaccharides-based materials are widely investigated as cement additives. Polysaccharides and modified polysaccharides (such as starch sulfonate and starch ether) have been used in the cement industry as a water-reducing (dispersing) additive or as a retarder. There are many publications on micron- and nano-cellulose enhanced cement. Results show a general enhancement of compressive strength and tensile strength

Figure 34: Reaction scheme of chemical pretreatment of chitin to introduce carboxylate groups into the surface of chitin via the TEMPO-mediated oxidation method.

while reports on rheological properties such as slurry consistency and setting time are limited. Research on chitin nanofibers or chitin nanocrystals enhanced cement is rare. Most of the research on chitin or chitosan is focused on micron size (or larger) chitin, chitosan, or its derivative polymers. Chitin at the micrometer level can be used as a retarder and chitosan and its derivative polymers can be used as additives in cement and concrete, such as superplasticizer, anti-dispersant, retarder, *etc*. Chitosan derivative polylactic acid can be used as an alkali silicic acid inhibitor for self-packing cement.

8 Conclusion

Many studies focus on the reinforcing mechanisms of carbon nanofibers and CNTs in cement; however, publications on the application of PNMs in cement are far less, and the mechanisms responsible for the cement composite bulk properties are not well understood. This is probably due to the relatively short history of utilizing PNMs as alternative reinforcement materials in cement. This review showed many more studies focusing on cellulose nanocrystals and nanofibers, but only a few studies are available on starch derivatives as reinforcement and other types of modifiers for cement. Furthermore, reports on the use of chitin nanomaterials in cement and concrete are rare. Therefore, the reinforcing mechanisms of these PNMs in cementitious materials are not well understood.

A comprehensive review of the effects of surface chemistry and other properties of PNMs on cement hydration and the performances of the hardened cement composites were summarized based on the published results. Hypothesis on the potential interaction of PNMs with cement was provided in this review based on studies of widely used superplasticizers with sulfate and carboxylate

groups. The effect of particle size, morphology, aspect ratio, and functional groups of PNMs on the cement mechanical properties and the potential responsible mechanisms were discussed with the goal of better understanding the following aspects.

- 1) The influence of surface chemistry of PNMs on the diffusion of cation compounds and cement hydration.
- 2) The diffusion and adsorption behaviors of cations in the cement pore solution in the presence of negatively or positively charged PNMs.
- 3) Interfacial interaction between cement and PNMs.
- 4) The influence of PNMs on the phase composition and chemical and crystalline structures of hydration products as well as characterization techniques to reliably characterize and evaluate these impacts.
- 5) The existence of combined effects of surface chemistry and nano-size/morphology of PNMs on the growth of hydration products and the microstructure of the hardened cement composites.
- 6) The relationship between the specific structural arrangements of hydration products in the presence of PNMs and the hydrated cement properties.

Addressing the above research questions will significantly improve our understanding of the effect of PNMs on the properties of nano-reinforced cementitious materials. In addition, it will contribute to the development of new approaches towards advanced, crack-free cement concrete materials.

Funding information: This work was funded by the Advanced Research Projects Agency-Energy (ARPA-E) program of the Department of Energy, grant Number DE-AR0001140.

Author contributions: All authors have accepted responsibility for the entire content of this manuscript and approved its submission.

Conflict of interest: The authors state no conflict of interest.

References

- [1] Mehta PK, Monteiro PJ. Concrete microstructure, properties and materials. 4th ed, New York: McGraw-Hill Education; 2014.
- Bernhardt D, James RI. US geological survey, Reston, [2] Virginia: Mineral Commodity Summary. 2020:1-200.
- Hooton RD, Bickley JA. Design for durability: The key to [3] improving concrete sustainability. Constr Build Mater. 2014;67:422-30. doi: 10.1016/j.conbuildmat.2013.12.016.
- [4] Ali MB, Saidur R, Hossain MS. A review on emission analysis in cement industries. Renew Sustain Energy Rev. 2011:15(5):2252-61. doi: 10.1016/i.rser.2011.02.014.
- [5] Hasanbeigi A, Price L, Lin E. Emerging energy-efficiency and CO₂ emission-reduction technologies for cement and concrete production: A technical review. Renew Sustain Energy Rev. 2012;16(8):6220-38. doi: 10.1016/j.rser.2012.07.019.
- [6] Rehan R, Nehdi M. Carbon dioxide emissions and climate change: policy implications for the cement industry. Environ Sci Policy. 2005;8(2):105-14. doi: 10.1016/ j.envsci.2004.12.006.
- [7] Worrell E, Price L, Martin N, Hendriks C, Meida LO. Carbon dioxide emissions from the global cement industry. Annu Rev Energy Environ. 2001;26(1):303-29. doi: 10.1146/ annurev.energy.26.1.303.
- [8] Yang K, Zhong M, Magee B, Yang C, Wang C, Zhu X, et al. Investigation of effects of Portland cement fineness and alkali content on concrete plastic shrinkage cracking. Constr Build Mater. 2017;144:279-90. doi: 10.1016/ j.conbuildmat.2017.03.130.
- Ghourchian S, Wyrzykowski M, Baquerizo L, Lura P. Susceptibility of Portland cement and blended cement concretes to plastic shrinkage cracking. Cem Concr Compos. 2018;85:44-55. doi: 10.1016/j.cemconcomp.2017.10.002.
- Pan Z, Sanjayan JG, Kong DLY. Effect of aggregate size on spalling of geopolymer and Portland cement concretes subjected to elevated temperatures. Constr Build Mater. 2012;36:365-72. doi: 10.1016/j.conbuildmat.2012.04.120.
- [11] Singh NB, Kalra M, Saxena SK. Nanoscience of cement and concrete. Mater Today Proc. 2017;4(4, Part E):5478-87. doi: 10.1016/j.matpr.2017.06.003.
- [12] Thomas JJ, Jennings HM, Chen JJ. Influence of nucleation seeding on the hydration mechanisms of tricalcium silicate and cement. J Phys Chem C. 2009;113(11):4327-34. doi: 10.1021/jp809811w.
- Cappelletto E, Borsacchi S, Geppi M, Ridi F, Fratini E, [13] Baglioni P. Comb-shaped polymers as nanostructure modifiers of calcium silicate hydrate: A ²⁹Si solid-state NMR investigation. J Phys Chem C. 2013;117(44):22947-53. doi: 10.1021/jp407740t.
- [14] Beaudoin JJ, Raki L, Alizadeh R. A 29Si MAS NMR study of modified C-S-H nanostructures. Cem Concr Compos. 2009;31(8):585-90. doi: 10.1016/ j.cemconcomp.2008.11.004.

- Yakovlev G, Kerienė J, Gailius A, Girnienė I. Cement based foam concrete reinforced by carbon nanotubes. Mater Sci. 2006;12(2):147-51. http://dspace1.vgtu.lt/handle/1/220.
- [16] Parveen S, Rana S, Fangueiro R. A review on nanomaterial dispersion, microstructure, and mechanical properties of carbon nanotube and nanofiber reinforced cementitious composites. J Nanomaterials. 2013;2013(80):80-119. doi: 10.1155/2013/710175.
- [17] Zhang M, Li H. Pore structure and chloride permeability of concrete containing nano-particles for pavement. Constr Build Mater. 2011;25(2):608-16. doi: 10.1016/ j.conbuildmat.2010.07.032.
- [18] Papatzani S, Paine K, Calabria-Holley J. A comprehensive review of the models on the nanostructure of calcium silicate hydrates. Constr Build Mater. 2015;74:219-34. doi: 10.1016/ j.conbuildmat.2014.10.029.
- Lepech MD, Li VC. Water permeability of cracked cementi-[19] tious composites. Proceedings of Eleventh International Conference on Fracture. Turin, Italy: Curran Associates, Inc. 2005. p. 20-5.
- [20] Li GY, Wang PM, Zhao X. Mechanical behavior and microstructure of cement composites incorporating surfacetreated multi-walled carbon nanotubes. Carbon. 2005;43(6):1239-45. doi: 10.1016/j.carbon.2004.12.017.
- [21] Xie X-L, Mai Y-W, Zhou X-P. Dispersion and alignment of carbon nanotubes in polymer matrix: A review. Mater Sci Engineering R Rep. 2005;49(4):89-112. doi: 10.1016/ j.mser.2005.04.002.
- [22] Ma P-C, Siddiqui NA, Marom G, Kim J-K. Dispersion and functionalization of carbon nanotubes for polymer-based nanocomposites: A review. Compos Part A Appl Sci Manuf. 2010;41(10):1345-67. doi: 10.1016/ j.compositesa.2010.07.003.
- [23] Mohammadkazemi F, Doosthoseini K, Ganjian E, Azin M. Manufacturing of bacterial nano-cellulose reinforced fiber -cement composites. Constr Build Mater. 2015;101:958-64. doi: 10.1016/j.conbuildmat.2015.10.093.
- [24] Hisseine OA, Wilson W, Sorelli L, Tolnai B, Tagnit-Hamou A. Nanocellulose for improved concrete performance: A macroto-micro investigation for disclosing the effects of cellulose filaments on strength of cement systems. Constr Build Mater. 2019;206:84-96. doi: 10.1016/j.conbuildmat.2019.02.042.
- [25] Akhlaghi MA, Bagherpour R, Kalhori H. Application of bacterial nanocellulose fibers as reinforcement in cement composites. Constr Build Mater. 2020;241:118061. doi: 10.1016/ j.conbuildmat.2020.118061.
- El Knidri H, Belaabed R, Addaou A, Laajeb A, Lahsini A. [26] Extraction, chemical modification and characterization of chitin and chitosan. Int J Biol Macromolecules. 2018;120:1181-9. doi: 10.1016/j.ijbiomac.2018.08.139.
- [27] Rolandi M, Rolandi R. Self-assembled chitin nanofibers and applications. Adv Colloid Interface Sci. 2014;207:216-22. doi: 10.1016/j.cis.2014.01.019.
- [28] Dewacker DR. Cement mortar systems using blends of polysaccharides and cold-water-soluble, unmodified starches. US5575840A; 1996. https://patents.google.com/patent/ US5575840A/en?oq = US5575840A.
- [29] Crépy L, Petit J-Y, Wirguin E, Martin P, Joly N. Synthesis and evaluation of starch-based polymers as potential dispersants in cement pastes and self leveling compounds.

- Cem Concr Compos. 2014;45:29-38. doi: 10.1016/j.cemconcomp.2013.09.004.
- [30] Moon RJ, Martini A, Nairn J, Simonsen J, Youngblood J. Cellulose nanomaterials review: structure, properties and nanocomposites. Chem Soc Rev. 2011;40(7):3941–94. doi: 10.1039/C0CS00108B.
- [31] Sjostrom E. Wood chemistry: Fundamentals and applications. Houston: Gulf Professional Publishing: 1993.
- [32] Azizi Samir MAS, Alloin F, Dufresne A. Review of recent research into cellulosic whiskers, their properties and their application in nanocomposite field. Biomacromolecules. 2005;6(2):612–26. doi: 10.1021/bm0493685.
- [33] Onuaguluchi O, Panesar DK, Sain M. Properties of nanofibre reinforced cement composites. Constr Build Mater. 2014;63:119–24. doi: 10.1016/j.conbuildmat.2014.04.072.
- [34] Sun X, Wu Q, Lee S, Qing Y, Wu Y. Cellulose nanofibers as a modifier for rheology, curing and mechanical performance of oil well cement. Sci Rep. 2016;6(1):31654. doi: 10.1038/ srep31654.
- [35] Sun X, Wu Q, Zhang J, Qing Y, Wu Y, Lee S. Rheology, curing temperature and mechanical performance of oil well cement: Combined effect of cellulose nanofibers and graphene nanoplatelets. Mater & Des. 2017;114:92–101. doi: 10.1016/ j.matdes.2016.10.050.
- [36] Hisseine OA, Basic N, Omran AF, Tagnit-Hamou A. Feasibility of using cellulose filaments as a viscosity modifying agent in self-consolidating concrete. Cem Concr Compos. 2018;94:327-40. doi: 10.1016/ j.cemconcomp.2018.09.009.
- [37] Haddad Kolour H. An investigation on the effects of cellulose nanofibrils on the performance of cement based composites. PhD Dissertation, Orono, Maine: The University of Maine; 2019. https://digitalcommons.library.umaine.edu/etd/ 3128/.
- [38] Bakkari ME, Bindiganavile V, Goncalves J, Boluk Y. Preparation of cellulose nanofibers by TEMPO-oxidation of bleached chemi-thermomechanical pulp for cement applications. Carbohydr Polym. 2019;203:238–45. doi: 10.1016/j.carbpol.2018.09.036.
- [39] Goncalves J, El-Bakkari M, Boluk Y, Bindiganavile V. Cellulose nanofibres (CNF) for sulphate resistance in cement based systems. Cem Concr Compos. 2019;99:100–11. doi: 10.1016/j.cemconcomp.2019.03.005.
- [40] Jiao L, Su M, Chen L, Wang Y, Zhu H, Dai H. Natural cellulose nanofibers as sustainable enhancers in construction cement. PLoS One. 2016;11(12):e0168422. doi: 10.1371/ journal.pone.0168422.
- [41] Mejdoub R, Hammi H, Suñol JJ, Khitouni M, M'nif A, Boufi S. Nanofibrillated cellulose as nanoreinforcement in Portland cement: Thermal, mechanical and microstructural properties. J Composite Mater. 2017;51(17):2491–503. doi: 10.1177/ 0021998316672090.
- [42] Cao Y, Zavaterri P, Youngblood J, Moon R, Weiss J. The influence of cellulose nanocrystal additions on the performance of cement paste. Cem Concr Compos. 2015;56:73–83. doi: 10.1016/j.cemconcomp.2014.11.008.
- [43] Cao Y, Tian N, Bahr D, Zavattieri PD, Youngblood J, Moon RJ, et al. The influence of cellulose nanocrystals on the microstructure of cement paste. Cem Concr Compos. 2016;74:164-73. doi: 10.1016/j.cemconcomp.2016.09.008.

- [44] Montes F, Fu T, Youngblood JP, Weiss J. Rheological impact of using cellulose nanocrystals (CNC) in cement pastes. Constr Build Mater. 2020;235:117497. doi: 10.1016/j.conbuildmat.2019.117497.
- [45] Dousti MR, Boluk Y, Bindiganavile V. The effect of cellulose nanocrystal (CNC) particles on the porosity and strength development in oil well cement paste. Constr Build Mater. 2019;205:456-62. doi: 10.1016/j.conbuildmat.2019.01.073.
- [46] Mazlan D, Krishnan S, Din MFM, Tokoro C, Khalid NHA, Ibrahim IS, et al. Effect of cellulose nanocrystals extracted from oil palm empty fruit bunch as green admixture for mortar. Sci Rep. 2020;10:6412. doi: 10.1038/s41598-020-63575-7.
- [47] Ong KJ, Shatkin JA, Nelson K, Ede JD, Retsina T. Establishing the safety of novel bio-based cellulose nanomaterials for commercialization. NanoImpact. 2017;6:19–29. doi: 10.1016/ j.impact.2017.03.002.
- [48] Habibi Y, Lucia LA, Rojas OJ. Cellulose nanocrystals: Chemistry, self-assembly, and applications. Chem Rev. 2010;110(6):3479-500. doi: 10.1021/cr900339w.
- [49] Battista OA, Coppick S, Howsmon JA, Morehead FF, Sisson WA. Level-off degree of polymerization. Ind Eng Chem. 1956;48(2):333-5. doi: 10.1021/ie50554a046.
- [50] Takaragi A, Minoda M, Miyamoto T, Liu HQ, Zhang LN. Reaction characteristics of cellulose in the LiCl/1,3-dimethyl-2-imidazolidinone solvent system. Cellulose. 1999;6(2):93-102. doi: 10.1023/A:1009208417954.
- [51] Lin N, Dufresne A. Nanocellulose in biomedicine: Current status and future prospect. Eur Polym J. 2014;59:302-25. doi: 10.1016/j.eurpolymj.2014.07.025.
- [52] Reid MS, Villalobos M, Cranston ED. Benchmarking cellulose nanocrystals: From the laboratory to industrial production. Langmuir. 2017;33(7):1583–98. doi: 10.1021/ acs.langmuir.6b03765.
- [53] Dufresne A. Nanocellulose: from nature to high performance tailored materials. Berlin, Boston: Walter de Gruyter GmbH & Co KG: 2017.
- [54] Saito T, Isogai A. TEMPO-mediated oxidation of native cellulose. The effect of oxidation conditions on chemical and crystal structures of the water-insoluble fractions. Biomacromolecules. 2004;5(5):1983-9. doi: 10.1021/bm0497769.
- [55] Isogai A, Saito T, Fukuzumi H. TEMPO-oxidized cellulose nanofibers. Nanoscale. 2011;3(1):71–85. doi: 10.1039/ CONR00583E.
- [56] Abe K, Yano H. Comparison of the characteristics of cellulose microfibril aggregates of wood, rice straw and potato tuber. Cellulose. 2009;16(6):1017-23. doi: 10.1007/s10570-009-9334-9.
- [57] de Assis CA, Iglesias MC, Bilodeau M, Johnson D, Phillips R, Peresin MS, et al. Cellulose micro- and nanofibrils (CMNF) manufacturing – financial and risk assessment. Biofuels Bioprod Bioref. 2018;12(2):251–64. doi: 10.1002/bbb.1835.
- [58] Iwamoto S, Nakagaito AN, Yano H. Nano-fibrillation of pulp fibers for the processing of transparent nanocomposites. Appl Phys A. 2007;89(2):461-6. doi: 10.1007/s00339-007-4175-6.
- [59] Chaker A, Alila S, Mutjé P, Vilar MR, Boufi S. Key role of the hemicellulose content and the cell morphology on the nanofibrillation effectiveness of cellulose pulps. Cellulose. 2013;20(6):2863-75. doi: 10.1007/s10570-013-0036-y.

- [60] Kurita K. Chemistry and application of chitin and chitosan. Polym Degrad Stab. 1998;59(1-3):117-20. doi: 10.1016/ 50141-3910(97)00160-2.
- [61] Rinaudo M. Chitin and chitosan: Properties and applications. Prog Polym Sci. 2006;31(7):603-32. doi: 10.1016/ j.progpolymsci.2006.06.001.
- Dong Y, Xu C, Wang J, Wu Y, Wang M, Ruan Y. Influence of degree of deacetylation on critical concentration of chitosan/ dichloroacetic acid liquid-crystalline solution. J Appl Polym Sci. 2002;83(6):1204-8. doi: 10.1002/app.2286.
- [63] Pillai CKS, Paul W, Sharma CP. Chitin and chitosan polymers: Chemistry, solubility and fiber formation. Prog Polym Sci. 2009;34(7):641-78. doi: 10.1016/ i.progpolymsci.2009.04.001.
- Fan Y, Saito T, Isogai A. Chitin nanocrystals prepared by TEMPO-mediated oxidation of α -chitin. Biomacromolecules. 2008;9(1):192-8. doi: 10.1021/bm700966g.
- Shinoda R, Saito T, Okita Y, Isogai A. Relationship between length and degree of polymerization of TEMPO-oxidized cellulose nanofibrils. Biomacromolecules. 2012;13(3):842-9. doi: 10.1021/bm2017542.
- Fan Y, Saito T, Isogai A. Individual chitin nano-whiskers [66] prepared from partially deacetylated α -chitin by fibril surface cationization. Carbohydr Polym. 2010;79(4):1046-51. doi: 10.1016/j.carbpol.2009.10.044.
- Zhong T, Wolcott MP, Liu H, Glandon N, Wang J. The influence [67] of pre-fibrillation via planetary ball milling on the extraction and properties of chitin nanofibers. Cellulose. 2020;27(11):6205-16. doi: 10.1007/s10570-020-03186-7.
- [68] Patural L, Marchal P, Govin A, Grosseau P, Ruot B, Devès O. Cellulose ethers influence on water retention and consistency in cement-based mortars. Cem Concr Res. 2011;41(1):46-55. doi: 10.1016/j.cemconres.2010.09.004.
- Peschard A, Govin A, Grosseau P, Guilhot B, Guyonnet R. Effect of polysaccharides on the hydration of cement paste at early ages. Cem Concr Res. 2004;34(11):2153-8. doi: 10.1016/j.cemconres.2004.04.001.
- Vieira MC, Klemm D, Einfeldt L, Albrecht G. Dispersing agents for cement based on modified polysaccharides. Cem Concr Res. 2005;35(5):883-90. doi: 10.1016/ j.cemconres.2004.09.022.
- [71] Zhang D-F, Ju B-Z, Zhang S-F, He L, Yang J-Z. The study on the dispersing mechanism of starch sulfonate as a water-reducing agent for cement. Carbohydr Polym. 2007;70(4):363-8. doi: 10.1016/j.carbpol.2007.04.024.
- Zhang H, Wang W, Li Q, Tian Q, Li L, Liu J. A starch-based admixture for reduction of hydration heat in cement composites. Constr Build Mater. 2018;173:317-22. doi: 10.1016/ j.conbuildmat.2018.03.199.
- [73] Claramunt J, Ventura H, Toledo Filho RD, Ardanuy M. Effect of nanocelluloses on the microstructure and mechanical performance of CAC cementitious matrices. Cem Concr Res. 2019;119:64-76. doi: 10.1016/j.cemconres.2019.02.006.
- Alzoubi HH, Albiss BA. Performance of cementitious compo-[74] sites with nano PCMs and cellulose nano fibers. Constr Build Mater. 2020;236:117483. doi: 10.1016/ j.conbuildmat.2019.117483.
- [75] Kamasamudram KS, Ashraf W, Landis EN. Cellulose nanofibrils with and without nanosilica for the performance enhancement of Portland cement systems. Constr

- Build Mater. 2021;285:121547. doi: 10.1016/ j.conbuildmat.2020.121547.
- [76] Nassiri S, Chen Z, Jian G, Zhong T, Haider MM, Li H, et al. Comparison of unique effects of two contrasting types of cellulose nanomaterials on setting time, rheology, and compressive strength of cement paste. Cem Concr Compos. 2021;123:104201. doi: 10.1016/j.cemconcomp.2021.104201.
- [77] Cuenca E, Mezzena A, Ferrara L. Synergy between crystalline admixtures and nano-constituents in enhancing autogenous healing capacity of cementitious composites under cracking and healing cycles in aggressive waters. Constr Build Mater. 2021;266:121447. doi: 10.1016/j.conbuildmat.2020.121447.
- [78] Flores J, Kamali M, Ghahremaninezhad A. An investigation into the properties and microstructure of cement mixtures modified with cellulose nanocrystal. Materials. 2017;10(5):498. doi: 10.3390/ma10050498.
- Mcalpine S, Nakoneshny J, Kunkel B. Crystalline cellulose [79] reinforced cement. US20200079692A1; 2020. https:// patents.google.com/patent/US20200079692A1/en?oq = US20200079692A1.
- [80] Barría JC, Vázquez A, Pereira J-M, Manzanal D. Effect of bacterial nanocellulose on the fresh and hardened states of oil well cement. J Pet Sci Eng. 2021;199:108259. doi: 10.1016/ j.petrol.2020.108259.
- [81] Tegiacchi F, Casu B. Alkylsulfonated polysaccharides and mortar and concrete mixes containing them. USH493H; 1988. https:// patents.google.com/patent/USH493H/en?oq = USH493H.
- [82] Yamamuro H. Property of new polysaccharide derivative as a viscosity agent for self-compacting concrete. Cachan, France: RILEM Publications; 1999. p. 449-59.
- [83] Wang X, Ma J, Wang Y, He B. Reinforcement of calcium phosphate cements with phosphorylated chitin. Chin J Polym Sci. 2002;20(4):325-32. http://www.cjps.org/article/id/ 112d256e-9075-421e-bbf3-f9165b56e2b0?pageType = en.
- Pourchez J, Peschard A, Grosseau P, Guyonnet R, Guilhot B, [84] Vallée F. HPMC and HEMC influence on cement hydration. Cem Concr Res. 2006;36(2):288-94. doi: 10.1016/ j.cemconres.2005.08.003.
- [85] Roddy CW, Todd BL. Methods of cementing in subterranean formations using crack resistant cement compositions. US7036586B2; 2006. https://patents.google.com/patent/ US7036586B2/en?oq = US7036586B2.
- [86] Lasheras-Zubiate M, Navarro-Blasco I, Fernández JM, Alvarez JI. Studies on chitosan as an admixture for cementbased materials: Assessment of its viscosity enhancing effect and complexing ability for heavy metals. J Appl Polym Sci. 2011;120(1):242-52. doi: 10.1002/app.33048.
- [87] Lasheras-Zubiate M, Navarro-Blasco I, Fernández JM, Álvarez JI. Effect of the addition of chitosan ethers on the fresh state properties of cement mortars. Cem Concr Compos. 2012;34(8):964-73. doi: 10.1016/ j.cemconcomp.2012.04.010.
- [88] Cestari AR, Vieira EFS, Alves FJ, Silva ECS, Andrade MAS. A novel and efficient epoxy/chitosan cement slurry for use in severe acidic environments of oil wells-Structural characterization and kinetic modeling. J Hazard Mater. 2012;213-214:109-16. doi: 10.1016/j.jhazmat.2012.01.068.
- [89] Reddy BR, Ghosh A, Fitzgerald R. Polysaccharide based cement additives. US8586508B2; 2013. https://patents. google.com/patent/US8586508B2/en?oq = US8586508B2.

- Vieira EFS, Lima PF, dos Santos IMG, Mangrich AS, de França AA, Le Saoût G, et al. The influence of in situ polymerized epoxidized A/F bisphenol-chitosan on features of oil well cement slurry-Molecular-level analysis and long-term interaction of API fracturing fluid. J Appl Polym Sci. 2014;131(22):41044. doi: 10.1002/app.41044.
- Lv S, Liu J, Zhou Q, Huang L, Sun T. Synthesis of modified chitosan superplasticizer by amidation and sulfonation and its application performance and working mechanism. Ind Eng Chem Res. 2014;53(10):3908-16. doi: 10.1021/ ie403786q.
- Isik IE, Ozkul MH. Utilization of polysaccharides as viscosity modifying agent in self-compacting concrete. Constr Build Mater. 2014:72:239-47. doi: 10.1016/ j.conbuildmat.2014.09.017.
- [93] Liu H, Bu Y, Sanjayan J, Shen Z. Effects of chitosan treatment on strength and thickening properties of oil well cement. Constr Build Mater. 2015;75:404-14. doi: 10.1016/ j.conbuildmat.2014.11.047.
- [94] Liu H, Bu Y, Bu C, Guo S. A kind of pre-chelating chitosan cementing slurry retardant and preparation method thereof. CN103045213B; 2015. https://patents.google.com/patent/ CN103045213B/en?oq = CN103045213B.
- [95] Ustinova YV, Nikiforova TP. Cement compositions with the chitosan additive. Procedia Eng. 2016;153:810-5. doi: 10.1016/j.proeng.2016.08.247.
- [96] Zhao H, Chen D, Liao Y, Ouyang F, Du Y, Xu H. A kind of preparation method of the modified chitin bio-based efficient retarding and water reducing agent containing carboxyl. CN107601945A; 2018. https://patents.google.com/patent/ CN107601945A/en?oq = CN107601945A.
- Wang J, Mignon A, Trenson G, Van Vlierberghe S, Boon N, De, et al. A chitosan based pH-responsive hydrogel for encapsulation of bacteria for self-sealing concrete. Cem Concr Compos. 2018;93:309-22. doi: 10.1016/ j.cemconcomp.2018.08.007.
- [98] Hall LJ. Chitin nanocrystal containing wellbore fluids. US10259981B2; 2019. https://patents.google.com/patent/ US10259981B2/en?og = US10259981B2.
- [99] Arslan H, Aytaç US, Bilir T, Şen Ş. The synthesis of a new chitosan based superplasticizer and investigation of its effects on concrete properties. Constr Build Mater. 2019;204:541-9. doi: 10.1016/j.conbuildmat.2019.01.209.
- [100] Zhao H, Chen D, Liao Y, Xuan W, Ouyang F, Feng J. A kind of high additive of low alkali_silica reaction expansion is discarded to crush glass self-compacting concrete preparation method. CN109534745A; 2019. https://patents.google.com/ patent/CN109534745A/en?oq = CN109534745A.
- [101] Zhao H, Chen D, Liao Y, Ouyang F, Xuan W, Xu H. Preparation method of modified natural chitin-acrylic acid copolymerized multifunctional organic anti-dispersant for underwater undispersed concrete. CN110922532A; 2020. https:// patents.google.com/patent/CN110922532A/en?oq = CN110922532A.
- [102] Zhao S, Liu Z, Mu Y, Wang F, He Y. Effect of chitosan on the carbonation behavior of γ -C₂S. Cem Concr Compos. 2020;111:103637. doi: 10.1016/j.cemconcomp.2020.103637.
- [103] Haider MM, Jian G, Zhong T, Li H, Fernandez CA, Fifield LS, et al. Insights into setting time, rheological and mechanical properties of chitin nanocrystals- and chitin nanofibers-

- cement paste. Cem Concr Compos. 2022;132:104623-41. doi: 10.1016/j.cemconcomp.2022.104623.
- [104] Zingg A, Winnefeld F, Holzer L, Pakusch J, Becker S, Gauckler L. Adsorption of polyelectrolytes and its influence on the rheology, zeta potential, and microstructure of various cement and hydrate phases. J Colloid Interface Sci. 2008;323(2):301-12. doi: 10.1016/j.jcis.2008.04.052.
- [105] John E, Matschei T, Stephan D. Nucleation seeding with calcium silicate hydrate - A review. Cem Concr Res. 2018;113:74-85. doi: 10.1016/j.cemconres.2018.07.003.
- [106] Hou D, Zhu Y, Lu Y, Li Z. Mechanical properties of calcium silicate hydrate (C-S-H) at nano-scale: A molecular dynamics study. Mater Chem Phys. 2014;146(3):503-11. doi: 10.1016/i.matchemphys.2014.04.001.
- [107] Joseph S, Bishnoi S, Balen KV, Cizer Ö. Modeling the effect of fineness and filler in early-age hydration of tricalcium silicate. J Am Ceram Soc. 2017;100(3):1178-94. doi: 10.1111/ jace.14676.
- [108] Taylor HF. Cement chemistry. Vol. 2. London: Thomas Telford; 1997.
- [109] Pelleng RJ, Kushima A, Shahsavari R, Van Vliet KJ, Buehler MJ, Yip S, et al. A realistic molecular model of cement hydrates. PNAS. 2009;106(38):16102-7. doi: 10.1073/ pnas.0902180106.
- [110] Kunhi Mohamed A, Parker SC, Bowen P, Galmarini S. An atomistic building block description of C-S-H - Towards a realistic C-S-H model. Cem Concr Res. 2018;107:221-35. doi: 10.1016/j.cemconres.2018.01.007.
- [111] Cho BH, Chung W, Nam BH. Molecular dynamics simulation of calcium-silicate-hydrate for nano-engineered cement composites—a review. Nanomaterials. 2020;10(11):2158. doi: 10.3390/nano10112158.
- [112] Jennings HM, Bullard JW, Thomas JJ, Andrade JE, Chen JJ, Scherer GW. Characterization and modeling of pores and surfaces in cement paste. J Adv Concr Technol. 2008;6(1):5-29. doi: 10.3151/jact.6.5.
- [113] Garboczi EJ, Bentz DP. The effect of statistical fluctuation, finite size error, and digital resolution on the phase percolation and transport properties of the NIST cement hydration model. Cem Concr Res. 2001;31(10):1501-14. doi: 10.1016/ S0008-8846(01)00593-2.
- [114] Nonat A. The structure and stoichiometry of C-S-H. Cem Concr Res. 2004;34(9):1521-8. doi: 10.1016/ j.cemconres.2004.04.035.
- [115] Richardson IG. Tobermorite/jennite- and tobermorite/calcium hydroxide-based models for the structure of C-S-H: applicability to hardened pastes of tricalcium silicate, βdicalcium silicate, Portland cement, and blends of Portland cement with blast-furnace slag, metakaolin, or silica fume. Cem Concr Res. 2004;34(9):1733-77. doi: 10.1016/ j.cemconres.2004.05.034.
- Kendall K, Howard AJ, Birchall JD, Pratt PL, Proctor BA, [116] Jefferis SA, et al. The relation between porosity, microstructure and strength, and the approach to advanced cementbased materials. Philos Trans R Soc Lond. 1983;310(1511):139-53. doi: 10.1098/rsta.1983.0073.
- [117] Balea A, Fuente E, Blanco A, Negro C. Nanocelluloses: Natural-based materials for fiber-reinforced cement composites. A critical review. Polymers. 2019;11(3):518. doi: 10.3390/polym11030518.

- [118] Jennings HM. A model for the microstructure of calcium silicate hydrate in cement paste. Cem Concr Res. 2000;30(1):101-16. doi: 10.1016/S0008-8846(99)00209-4.
- [119] Jennings HM, Thomas JJ, Gevrenov JS, Constantinides G, Ulm F-J. A multi-technique investigation of the nanoporosity of cement paste. Cem Concr Res. 2007;37(3):329-36. doi: 10.1016/j.cemconres.2006.03.021.
- [120] Dalas F, Nonat A, Pourchet S, Mosquet M, Rinaldi D, Sabio S. Tailoring the anionic function and the side chains of comblike superplasticizers to improve their adsorption. Cem Concr Res. 2015;67:21-30. doi: 10.1016/j.cemconres.2014.07.024.
- [121] Liu J, Yu C, Shu X, Ran Q, Yang Y. Recent advance of chemical admixtures in concrete. Cem Concr Res. 2019;124:105834. doi: 10.1016/j.cemconres.2019.105834.
- [122] Zhao H, Yang Y, Shu X, Wang Y, Wu S, Ran Q, et al. The binding of calcium ion with different groups of superplasticizers studied by three DFT methods, B3LYP, M06-2X and M06. Computational Mater Sci. 2018;152:43-50. doi: 10.1016/j.commatsci.2018.05.034.
- [123] Ilg M, Plank J. Non-adsorbing small molecules as auxiliary dispersants for polycarboxylate superplasticizers. Colloids Surf A Physicochemical Eng Asp. 2020;587:124307. doi: 10.1016/j.colsurfa.2019.124307.
- [124] Lewis JA, Matsuyama H, Kirby G, Morissette S, Young JF. Polyelectrolyte effects on the rheological properties of concentrated cement suspensions. J Am Ceram Soc. 2000;83(8):1905-13. doi: 10.1111/j.1151-2916.2000.tb01489.x.
- [125] Plank J, Sachsenhauser B. Experimental determination of the effective anionic charge density of polycarboxylate superplasticizers in cement pore solution. Cem Concr Res. 2009;39(1):1-5. doi: 10.1016/j.cemconres.2008.09.001.
- [126] Flatt R, Schober I. 7 Superplasticizers and the rheology of concrete. Understanding the Rheology of Concrete. Cambridge, UK: Woodhead Publishing; 2012. p. 144-208. doi: 10.1533/9780857095282.2.144.
- [127] von Hoessle F, Plank J, Leroux F. Intercalation of sulfonated melamine formaldehyde polycondensates into a hydrocalumite LDH structure. J Phys Chem Solids. 2015;80:112-7. doi: 10.1016/j.jpcs.2015.01.008.
- [128] Yoshioka K, Sakai E, Daimon M, Kitahara A. Role of steric hindrance in the performance of superplasticizers for concrete. J Am Ceram Soc. 1997;80(10):2667-71. doi: 10.1111/ j.1151-2916.1997.tb03169.x.
- [129] Lv S, Ju H, Qiu C, Ma Y, Zhou Q. Effects of connection mode between carboxyl groups and main chains on polycarboxylate superplasticizer properties. J Appl Polym Sci. 2013;128(6):3925-32. doi: 10.1002/app.38608.
- [130] Lv S, Cao Q, Zhou Q, Lai S, Gao F. Structure and characterization of sulfated chitosan superplasticizer. J Am Ceram Soc. 2013;96(6):1923-9. doi: 10.1111/jace.12221.
- [131] Goncalves J, Boluk Y, Bindiganavile V. Cellulose nanofibres mitigate chloride ion ingress in cement-based systems. Cem Concr Compos. 2020;114:103780. doi: 10.1016/ j.cemconcomp.2020.103780.
- [132] Côté AP, Shimizu GKH. The supramolecular chemistry of the sulfonate group in extended solids. Coord Chem Rev. 2003;245(1-2):49-64. doi: 10.1016/S0010-8545(03) 00033-X.

- [133] Zhao H, Yang Y, Wang Y, Shu X, Wu S, Ran Q, et al. Binding of calcium cations with three different types of oxygen-based functional groups of superplasticizers studied by atomistic simulations. J Mol Model. 2018;24(11):321. doi: 10.1007/ s00894-018-3853-y.
- [134] Guibal E. Interactions of metal ions with chitosan-based sorbents: a review. Sep Purif Technol. 2004;38(1):43-74. doi: 10.1016/j.seppur.2003.10.004.
- [135] Ogawa K, Oka K, Yui T. X-ray study of chitosan-transition metal complexes. Chem Mater. 1993;5(5):726-8. doi: 10.1021/cm00029a026.
- [136] Hsien T-Y, Rorrer GL. Effects of acylation and crosslinking on the material properties and cadmium ion adsorption capacity of porous chitosan beads. Sep Sci Technol. 1995;30(12):2455-75. doi: 10.1080/01496399508021395.
- [137] Rhazi M, Desbrières J, Tolaimate A, Rinaudo M, Vottero P, Alagui A, et al. Influence of the nature of the metal ions on the complexation with chitosan.: Application to the treatment of liquid waste. Eur Polym J. 2002;38(8):1523-30. doi: 10.1016/ S0014-3057(02)00026-5.
- [138] Vold IMN, Vårum KM, Guibal E, Smidsrød O. Binding of ions to chitosan-selectivity studies. Carbohydr Polym. 2003;54(4):471-7. doi: 10.1016/j.carbpol.2003.07.001.
- [139] Flatt RJ, Houst YF. A simplified view on chemical effects perturbing the action of superplasticizers. Cem Concr Res. 2001;31(8):1169-76. doi: 10.1016/S0008-8846(01)00534-8.
- Gartner E, Maruyama I, Chen J. A new model for the C-S-H phase formed during the hydration of Portland cements. Cem Concr Res. 2017;97:95-106. doi: 10.1016/ j.cemconres.2017.03.001.
- [141] Wang F, Kong X, Wang D, Wang Q. The effects of nano-C-S-H with different polymer stabilizers on early cement hydration. J Am Ceram Soc. 2019;102(9):5103-16. doi: 10.1111/ iace.16425.
- [142] Sun J, Shi H, Qian B, Xu Z, Li W, Shen X. Effects of synthetic C-S-H/PCE nanocomposites on early cement hydration. Constr Build Mater. 2017;140:282-92. doi: 10.1016/ j.conbuildmat.2017.02.075.
- [143] Berodier E, Scrivener K. Understanding the filler effect on the nucleation and growth of C-S-H. J Am Ceram Soc. 2014;97(12):3764-73. doi: 10.1111/jace.13177.
- [144] Ardanuy Raso M, Claramunt Blanes J, Arévalo Peces R, Parés Sabatés F, Aracri E, Vidal Lluciá T. Nanofibrillated cellulose (NFC) as a potential reinforcement for high performance cement mortar composites. BioResources. 2012;7(3):3883-94. https://upcommons.upc.edu/handle/ 2117/16392.
- [145] Rosato L, Stefanidou M, Milazzo G, Fernandez F, Livreri P, Muratore N, et al. Study and evaluation of nano-structured cellulose fibers as additive for restoration of historical mortars and plasters. Mater Today Proc. 2017;4(7, Part 1):6954-65. doi: 10.1016/j.matpr.2017.07.025.
- Liew KM, Kai MF, Zhang LW. Carbon nanotube reinforced [146] cementitious composites: An overview. Compos Part A Appl Sci Manuf. 2016;91:301-23. doi: 10.1016/ j.compositesa.2016.10.020.
- da Costa Correia V, Santos SF, Soares Teixeira R, Savastano Junior H. Nanofibrillated cellulose and cellulosic pulp for reinforcement of the extruded cement based materials.

- Constr Build Mater. 2018;160:376-84. doi: 10.1016/ j.conbuildmat.2017.11.066.
- [148] Peters SJ, Rushing TS, Landis EN, Cummins TK. Nanocellulose and microcellulose fibers for concrete. Transportation Res Rec. 2010;2142(1):25-8. doi: 10.3141/2142-04.
- [149] Xu X, Liu F, Jiang L, Zhu JY, Haagenson D, Wiesenborn DP. Cellulose nanocrystals vs. cellulose nanofibrils: A comparative study on their microstructures and effects as polymer reinforcing agents. ACS Appl Mater Interfaces. 2013;5(8):2999-3009. doi: 10.1021/am302624t.
- [150] Cuenca E, D'Ambrosio L, Lizunov D, Tretjakov A, Volobujeva O, Ferrara L. Mechanical properties and selfhealing capacity of ultra high performance fibre reinforced
- concrete with alumina nano-fibres: Tailoring ultra high durability concrete for aggressive exposure scenarios. Cem Concr Compos. 2021;118:103956. doi: 10.1016/ j.cemconcomp.2021.103956.
- [151] Cao Y, Zavattieri P, Youngblood J, Moon R, Weiss J. The relationship between cellulose nanocrystal dispersion and strength. Constr Build Mater. 2016;119:71-9. doi: 10.1016/ j.conbuildmat.2016.03.077.
- [152] Khanjani P, Kosonen H, Ristolainen M, Virtanen P, Vuorinen T. Interaction of divalent cations with carboxylate group in TEMPO-oxidized microfibrillated cellulose systems. Cellulose. 2019;26(8):4841-51. doi: 10.1007/s10570-019-02417-w.